Colloquium: Phase diagram of strongly interacting matter

P. Braun-Munzinger and J. Wambach

GSI Helmholtzzentrum für Schwerionenforschung mbH, Planckstasse 1, D64291 Darmstadt, Germany and Technical University Darmstadt, Schlossgartenstrasse 9, D64287 Darmstadt, Germany

A fundamental question of physics is what ultimately happens to matter as it is heated or compressed. In the realm of very high temperature and density the fundamental degrees of freedom of the strong interaction, quarks and gluons, come into play and a transition from matter consisting of confined baryons and mesons to a state with "liberated" quarks and gluons is expected. The study of the possible phases of strongly interacting matter is at the focus of many research activities worldwide. In this paper the physical aspects of the phase diagram, its relation to the evolution of the early Universe, as well as the inner core of neutron stars are discussed. Also recent progress in the experimental study of hadronic or quark-gluon matter under extreme conditions with ultrarelativistic nucleus-nucleus collisions is summarized.

CONTENTS

I. INTRODUCTION

Matter that surrounds us comes in a variety of phases which can be transformed into each other by a change of external conditions such as temperature, pressure, composition etc. Transitions from one phase to another are often accompanied by drastic changes in the physical properties of a material, such as its elastic properties, light transmission, or electrical conductivity. A good example is water whose phases are (partly) accessible to everyday experience. Changes in external pressure and temperature result in a rich phase diagram which, besides the familiar liquid and gaseous phases, features a variety of solid (ice) phases in which the H_2O molecules arrange themselves in spatial lattices of certain symmetries (Fig. 1).

Twelve such crystalline (ice) phases are known at present. In addition, three amorphous (glass) phases have been identified. Well known points in the phase diagram are the triple point where the solid, liquid, and gas phases coexist and the critical end point at which there is no distinction between the liquid and gas phase. This is the end point of a line of first-order liquid-gas transitions; at this point the transition is of second order.

Under sufficient heating water, and for that matter any other substance, goes over into a new state, a "plasma," consisting of ions and free electrons. This transition is mediated by molecular or atomic collisions. It is continuous[1] and hence not a phase transition in the strict thermodynamic sense. On the other hand, the plasma exhibits new collective phenomena such as screening and "plasma oscillations" (Mrowczynski and Thoma, 2007). Plasma states can also be induced by high compression, where electrons are delocalized from their orbitals and form a conducting "degenerate" quantum plasma. In contrast to a hot plasma there exists in this case a true phase transition, the "metal-insulator" transition (Mott, 1968; Gebhard, 1997). Good examples are white dwarfs, stars at the end of their evolution which are stabilized by the degeneracy pressure of free electrons (Chandrasekhar, 1931; Shapiro and Teukolsky, 1983).

One may ask what ultimately happens when matter is heated and compressed. This is not a purely academic question but is of relevance for the early stages of the Universe as we go backwards in time in the cosmic evolution. Also the properties of dense matter are important for our understanding of the composition and properties of the inner core of neutron stars, the densest cosmic objects. Here the main players are no longer forces of electromagnetic origin but the strong interaction, which is responsible for the binding of protons and neutrons into nuclei and of quarks and gluons into hadrons. In the standard model of particle physics the

---

[1]Under certain conditions there may also be a true plasma phase transition, for recent evidence see Fortov *et al.* (2007).
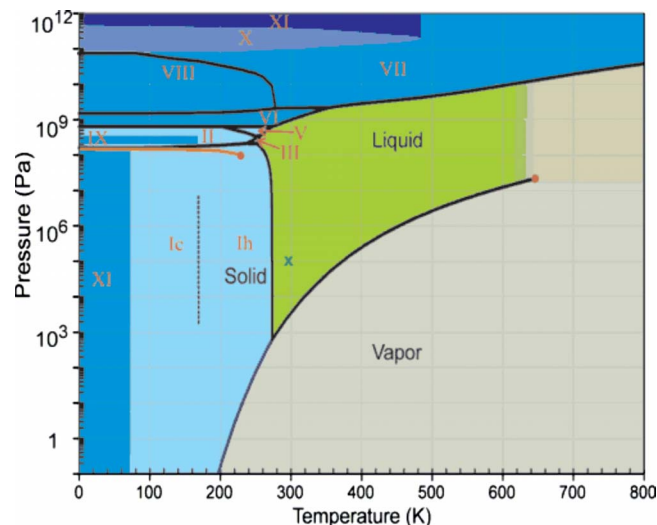
FIG. 1. (Color online) The phase diagram of H_2O (Chaplin, 2007). Besides the liquid and gaseous phases a variety of crystalline and amorphous phases occurs. Of special importance in the context of strongly interacting matter is the critical end point between the vapor and liquid phase.

strong interaction is described in the framework of a relativistic quantum field theory called quantum chromodynamics (QCD), where pointlike quarks and gluons are the elementary constituents.

The question of the fate of matter at very high temperature was first addressed by Hagedorn (1965) and later elaborated by Frautschi (1971). The analysis was based on the (pre-QCD) "bootstrap model" in which strongly interacting particles (hadrons) were viewed as composite "resonances" of lighter hadrons. A natural consequence of this model is the exponential growth in the density of mass states

$$\rho(M_h) \propto M_h^{-5/2} e^{M_h/T_H}. \tag{1}$$

This is verified by summing up the hadronic states listed by the Particle Data Group (Yao *et al.*, 2006). A fit to the data yields $T_H \sim 160-180$ MeV. It is then easy to see that the logarithm of the partition function of such a "resonance gas,"

$$\ln \mathcal{Z}^{RG}(T) = \sum_i \ln \mathcal{Z}_i^{RG} + \kappa \int_{m_0}^{\infty} dM_h \rho(M_h) M_h^{3/2} e^{-M_h/T}, \tag{2}$$

and, hence, all thermodynamic quantities diverge when $T = T_H$, which implies that matter cannot be heated beyond this limiting "Hagedorn temperature." Here $\ln \mathcal{Z}_i$ is the logarithm of the partition function for all well isolated particles with mass m_i. Above a certain mass m_0 all particles start to overlap and from that point on the sum is converted into an integral over the mass density $\rho(m)$ and all particles can be treated in the Boltzmann approximation. For the present argument the explicit value of the constant κ is immaterial. The energy supplied is used entirely for the production of new particles. This is of course at variance with our present understanding of

the big bang in which the temperature is set by the Planck scale $T \sim M_{\text{Planck}} = \sqrt{\hbar c / G_N} = 1.22 \times 10^{19}$ GeV, where the Planck mass is the mass for which the Schwarzschild radius is equal to the Compton length divided by π. The quantity G_N is the Newtonian gravitational constant and c is the speed of light.[2] Referring to the Hagedorn paper and the Friedman model of cosmology, Huang and Weinberg (Huang and Weinberg, 1970) speculated in 1970 about a limiting temperature also in the big bang but noted: "Our present theoretical apparatus is really inadequate to deal with much earlier times, say when $T > 100$ MeV."

The situation changed in the early and mid-1970s after it became clear that hadrons are built from quarks and gluons and hence have substructure. In this context Itoh proposed in 1970 that there might exist stars that are entirely made of very massive quarks, rather than ordinary baryons (Itoh, 1970).[3] The paradox of Hagedorn was taken up in 1975 (Cabibbo and Parisi, 1975; Collins and Perry, 1975) when it was noted that the quark-gluon substructure of hadrons opened the possibility for a phase transition to a new state of deconfined quark-gluon matter, called the "quark-gluon plasma."[4] In close analogy to Fisher's droplet model (Fisher, 1967) for phase transitions, Cabibbo and Parisi sketched a very simple (second-order) phase boundary for the quark-hadron transition. They argued that when matter is sufficiently heated or compressed, finite-size hadrons begin to overlap and quarks and gluons can travel freely over large space-time distances. Within this picture, the limiting temperature T_H is in reality close to or even coincides with the critical temperature for the phase transition between hadrons and quarks and gluons. With pointlike quarks and gluons the temperature in the early Universe can grow beyond bounds (big bang singularity).

II. STRONGLY INTERACTING MATTER UNDER EXTREME CONDITIONS

A. Quantum chromodynamics

To understand the salient features of the quark-hadron transition and to appreciate the historical developments in its physical understanding we need to recall some basic facts about the strong interaction. Its modern theory is quantum chromodynamics, introduced in 1973 (Fritzsch *et al.*, 1973). This relativistic field theory is formulated in close analogy to quantum electrodynamics (QED) as a gauge theory of massive fermionic matter fields interacting with massless bosonic gauge fields. In QED the Lagrangian density for the interaction of electrons with photons is given by

---

[2] In all formulas we use $\hbar = c = 1$.
[3] At that time quarks were considered very heavy to account for the fact that no free quarks were observed.
[4] This term was coined by Shuryak (1978).

$$\mathcal{L}_{\text{QED}} = -\tfrac{1}{4}F_{\mu\nu}F^{\mu\nu} + \bar{\psi}\gamma^{\mu}i(\partial_{\mu} + ieA_{\mu})\psi - m_e\bar{\psi}\psi, \qquad (3)$$

where $F_{\mu\nu}$ denotes the field strength tensor of the electromagnetic field, which in terms of the vector potential A_{μ} is obtained as

$$F_{\mu\nu} = \partial_{\mu}A_{\nu} - \partial_{\nu}A_{\mu}. \qquad (4)$$

The electrons are represented by the four-component Dirac spinor field ψ of mass m_e and the electric charge e denotes the fundamental coupling constant. The Lagrangian is invariant under simultaneous (local) gauge transformations of the fermion field of the electron and the vector potential

$$\psi \to e^{-i\chi}\psi, \quad A_{\mu} \to A_{\mu} + (i/e)\partial_{\mu}\chi, \qquad (5)$$

where $\chi(x)$ is a space-time-dependent real-valued function. The phase factor $e^{-i\chi}$ is an element of the unitary group U(1), which is hence called the "gauge group" of QED.

Because of the smallness of the fine structure constant $\alpha = e^2/4\pi \sim 1/137$ the evaluation of physical processes can be carried out in perturbation theory with high accuracy (the calculated value for the magnetic moment of the electron agrees to experiment within ten decimals). Historically this was one of the great triumphs of relativistic field theories.

In QCD, quarks and gluons are the elementary degrees of freedom. Aside from the relativistic quantum numbers dictated by Lorentz invariance, quarks come in six "flavors" (up, down, strange, charm, bottom, and top). To obtain the correct quantum statistics for hadronic wave functions it turns out that quarks as well as gluons also have to carry "color" as an additional quantum number (Nambu, 1960; Greenberg, 1964). The resulting Lagrangian density is then given by

$$\mathcal{L}_{\text{QCD}} = -\frac{1}{4}G^a_{\mu\nu}G^{\mu\nu}_a + \bar{q}\gamma^{\mu}i\left(\partial_{\mu} + ig_s\frac{\lambda_a}{2}A^a_{\mu}\right)q - m_q\bar{q}q, \qquad (6)$$

where q includes the flavor and color quantum numbers to be appropriately summed over. The strong coupling constant g_s is the analog of the electric charge e and m_q denotes the quark mass of a given flavor. These masses are generated in the electroweak sector of the standard model via the Higgs mechanism, first introduced in the context of superconductivity. We will return to this point and its physical implications later. The gauge group structure is more complicated than in QED since three colors are required for each quark.[5] For group theoretical consistency also gluons, the force carriers of the strong interaction, have to carry color charge (there are eight vector potentials A^a_{μ} instead of one). As a physical consequence they will self-interact. Mathematically this is reflected by a modification of the field strength tensor

$$G^{\mu\nu}_a = \partial^{\mu}A^{\nu}_a - \partial^{\nu}A^{\mu}_a - g_s f_{abc}A^{\mu}_b A^{\nu}_c, \qquad (7)$$

which now includes a nonlinear term. Its form is entirely dictated by the gauge group [which is now SU(3) rather than U(1)] through its structure constants f_{abc}.[6] The group structure is also reflected in the quark-gluon coupling through the Gell-Mann matrices λ_a which are the analog of the SU(2) Pauli matrices. Denoting the group of elements SU(3) by $U(\chi^a) \equiv e^{-i\chi^a\lambda_a/2}$ and defining $A_{\mu} \equiv (\lambda_a/2)A^a_{\mu}$, the gauge transformation corresponding to Eq. (5) now reads

$$q \to U(\chi^a)q,$$

$$A_{\mu} \to U(\chi^a)A_{\mu}U^{-1}(\chi^a) + \frac{i}{g_s}[\partial_{\mu}U(\chi^a)]U^{-1}(\chi^a). \qquad (8)$$

It reproduces QED for the gauge group U(1).

The more elaborate group structure renders QCD much more complicated than QED even at the classical level of Maxwell's equations.[7]

In any relativistic field theory the vacuum itself behaves, due to quantum fluctuations, like a polarizable medium. In QED the photon, although uncharged, can create virtual electron-positron pairs, causing partial screening of the charge of a test electron. This implies that the dielectric constant of the QED vacuum obeys[8] $\epsilon_0 > 1$. On the other hand, because of Lorentz invariance, $\epsilon_0\mu_0 = 1$, i.e., the magnetic permeability μ_0 is smaller than unity. Thus the QED vacuum behaves like a diamagnetic medium. In QCD, however, the gluons carry color charge as well as spin. In addition to virtual quark-antiquark pairs, which screen a color charge and thus would make the vacuum diamagnetic, the self-interaction of gluons can cause a color magnetization of the vacuum and make it paramagnetic. This effect actually overcomes the diamagnetic contribution from $\bar{q}q$ pairs such that $\mu^c_0 > 1$. The situation is somewhat similar to the paramagnetism of an electron gas, where the intrinsic spin alignment of electrons overwhelms the diamagnetism of orbital motion. Since $\mu^c_0 > 1$ it follows that $\epsilon^c_0 < 1$, so that the color-electric interaction between charged objects becomes stronger as their separation grows ("infrared slavery"). In this sense the QCD vacuum is an "antiscreening" medium. As the distance $r \to 0$, on the other hand, μ^c_0 and $\epsilon^c_0 \to 1$, and the interaction becomes weaker ("asymptotic freedom"). This gives

---

[5]Quarks form a fundamental representation of the Lie group SU(3).

[6]Gauge groups other than U(1) were first discussed by Yang and Mills (1954) in the context of SU(2) and the corresponding field theories are therefore called Yang-Mills theories. Since the generators of SU(N) do not commute, such theories are also called "non-Abelian."

[7]For instance, the wave equation for the vector potentials A^a_{μ} is nonlinear and its solutions in Euclidean space-time include solitons called "instantons."

[8]Provided the distance r is large enough so that the virtual cloud around the test charge is not penetrated. The distance scale is set by the inverse Compton wavelength of the electron, which is very small.
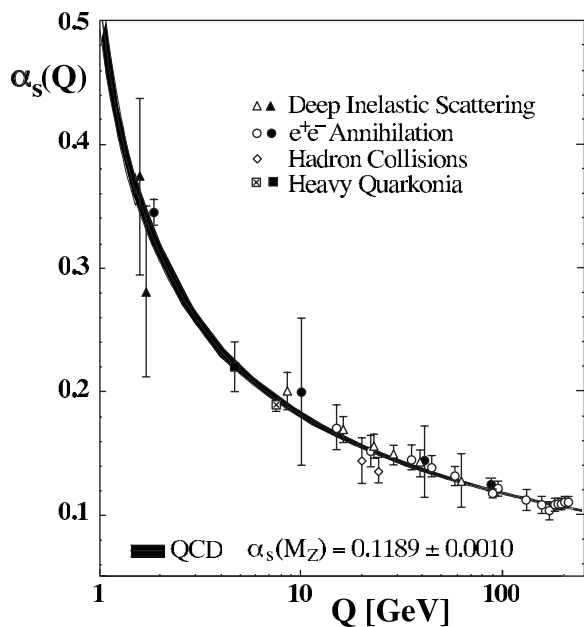
FIG. 2. The running of the fine structure constant of the strong interaction with the momentum transfer Q in a collision of quarks and/or gluons. From Bethke, 2007.

rise to a pronounced variation ("running") of the strong fine structure constant $\alpha_s = g_s^2/4\pi$ with (space-time) distance or momentum transfer Q. Its mathematical form to leading order was worked out in 1973 by Gross and Wilczek and independently by Politzer (Gross and Wilczek, 1973; Politzer, 1973) and reads

$$\alpha_s(Q^2) = \frac{12\pi}{(33 - 2N_f)\ln(Q^2/\Lambda^2_{\text{QCD}})}, \quad Q^2 \gg \Lambda^2_{\text{QCD}}, \quad (9)$$

where $\Lambda_{\text{QCD}} \approx 200$ MeV is the fundamental QCD scale parameter. As indicated in Fig. 2 the running of α_s is confirmed by experiments to very high precision and the authors were awarded the 2004 Nobel Prize in physics for their predictions. Even though a mathematical proof is still missing, it is generally believed that the strong increase in the coupling constant for low values of Q is responsible for the fact that isolated quarks and gluons have not been observed and are permanently "confined" in composite hadrons.

B. Models of the phase diagram

A simple picture of confinement is provided by the MIT-bag model (Chodos *et al.*, 1974). Here the idealized assumption is made that the QCD vacuum is a perfect paramagnet with $\mu_0^c = \infty$ and $\epsilon_0^c = 0$. A hadron is formed by carving a spherical cavity (bag) with radius $R \sim \Lambda_{\text{QCD}}^{-1} \approx 1$ fm out of the physical vacuum. Inside the bag the vacuum is trivial, i.e., $\mu_0^c = \epsilon_0^c = 1$, and the interaction between color charges is therefore weak. From the boundary conditions on the chromoelectric and chromomagnetic fields it immediately follows that the color

fields are totally confined within the hadron.[9] The cost in energy density for creating the cavity is called the bag constant B. After filling the bag with three quarks for baryons or quark-antiquark pairs for mesons and imposing appropriate boundary conditions on the quark wave functions to prevent leakage of color currents across the boundary, B can be determined from a fit to known hadron masses.

For the quark-hadron transition the MIT-bag model provides the following picture: When matter is heated, nuclei eventually dissolve into protons and neutrons (nucleons). At the same time light hadrons (preferentially pions) are created thermally, which increasingly fill the space between the nucleons. Because of their finite spatial extent the pions and other thermally produced hadrons begin to overlap with each other and with the bags of the original nucleons such that a network of zones with quarks, antiquarks, and gluons is formed. At a certain critical temperature T_c these zones fill the entire volume in a "percolation" transition. This new state of matter is the quark-gluon plasma (QGP). The vacuum becomes trivial and the elementary constituents are weakly interacting since $\mu_0^c = \epsilon_0^c = 1$ everywhere. There is, however, a fundamental difference to ordinary electromagnetic plasmas in which the transition is caused by ionization and therefore gradual. Because of confinement there can be no liberation of quarks and radiation of gluons below the critical temperature. Thus a relatively sharp transition with $\Delta T/T_c \ll 1$ is expected. We will return to this issue in the section on numerical solutions of QCD on a space-time lattice. A similar picture emerges when matter is strongly compressed. In this case the nucleons overlap at a critical number density n_c and form a cold degenerate QGP consisting mostly of quarks. This state may be realized in the inner core of neutron stars and its properties will be discussed later.

In the MIT-bag model thermodynamic quantities such as energy density and pressure can be calculated as a function of temperature and quark chemical potential[10] μ_q and the phase transition is inferred via the Gibbs construction of the phase boundary. Under the simplifying assumption of a free gas of massless quarks, antiquarks, and gluons in the QGP at fixed T and μ_q one obtains the pressure

---

[9]The situation is analogous to the case of a cavity in a perfect conductor (superconductor) with $\mu = 0, \epsilon = \infty$ except that the role of μ and ϵ are interchanged.

[10]In contrast to water, where the phase diagram is usually characterized by pressure and temperature, the number density is generally not conserved for relativistic systems. Therefore, the grand canonical ensemble with state variables temperature and quark chemical potential is used. For strong interactions μ_q ensures conservation of baryon number and $\mu_q > 0$ implies a nonvanishing net quark density n_q.

$$p_{\mathrm{QGP}}(T,\mu_q) = 37\frac{\pi^2}{90}T^4 + \mu_q^2 T^2 + \frac{\mu_q^4}{2\pi^2} - B. \qquad (10)$$

To the factor $37 = 16 + 21$, 16 gluonic (8×2), 12 quark ($3 \times 2 \times 2$), and 12 antiquark degrees of freedom contribute.[11] For quarks an additional factor of 7/8 accounts for the differences in Bose-Einstein and Fermi-Dirac statistics. The temperature dependence of the pressure follows a Stefan-Boltzmann law, in analogy to the black-body radiation of massless photons. The properties of the physical vacuum are taken into account by the bag constant B, which is a measure for the energy density of the vacuum. By construction, the quark-hadron transition in the MIT-bag model is of first order, implying that the phase boundary is obtained by the requirement that, at constant chemical potential, the pressure of the QGP is equal to that in the hadronic phase. For the latter the equation of state (EoS) of hadronic matter is needed. Taking for simplicity a gas of massless pions of three different charge states, which yields $p_\pi(T,\mu_q) = (3\pi^2/90)T^4$, a simple phase diagram emerges in which the hadronic phase is separated from the QGP by a first-order transition line. Taking for the bag constant the original MIT fit to hadronic masses $B = 57.5$ MeV/fm^3 one obtains $T_c \sim 100$ MeV at $\mu_q = 0$ and $\mu_c \sim 300$ MeV at vanishing temperature (Buballa, 2005).

These results imply a number of problems. On the one hand, the transition temperature is too small, as we have learned. We will come back to this in the next section. On the other hand, at $3\mu_q = \mu_b \sim M_N$ (mass of the nucleon $M_N = 939$ MeV), where homogeneous nuclear matter consisting of interacting protons and neutrons is formed, a cold QGP is energetically almost degenerate with normal nuclear matter. Both problems are, however, merely of a quantitative nature and can be circumvented by raising the value of B. More serious is the fact that, at large μ_q, a gas of nucleons because of its color neutrality is always energetically preferred to the QGP. The biggest problem is, however, that QCD has a number of other symmetries besides local gauge symmetry which it shares with QED. Most notable in the present context is chiral symmetry, which is exact in the limit of vanishing quark masses. For massless fermions their spin is aligned either parallel (right handed) or antiparallel (left handed) to the momentum. Chirality of a massless fermion is a Lorentz-invariant concept, i.e., left- (right-) handed particles remain left- (right-) handed in all reference frames.[12] For physical up and down quark masses of only a few MeV this limit is satisfied well when comparing them to typical hadronic mass scales such as the mass of the nucleon.[13] Exact chiral symmetry implies

that only quarks with the same helicity or chirality interact, i.e., the left-handed and right-handed worlds completely decouple. This means, in particular, that physical states of opposite parity must be degenerate in mass.

Similar to a ferromagnet, where rotational symmetry is spontaneously broken at low temperatures through spin alignment, the chiral symmetry of the strong interaction is also spontaneously broken in the QCD vacuum as a result of the strong increase of α_s at small momenta (Fig. 2). Empirical evidence is the absence of parity doublets in the mass spectrum of hadrons. Since massless quarks flip their helicity at the bag boundary the MIT-bag model massively violates chiral symmetry. For the thermodynamic considerations discussed so far this is unimportant, but for other aspects of the phase diagram chiral symmetry will be crucial.

There exist effective theories for the strong interaction which emphasize the aspects of chiral symmetry and its spontaneous breaking in the physical vacuum. One of the most thoroughly studied model in connection with the phase diagram dates back to early work by Nambu and Jona-Lasinio (NJL) (Nambu and Jona-Lasinio, 1961a, 1961b), before QCD was formulated. In its original formulation the NJL model was a relativistic field theory for interacting pointlike nucleons of vanishing mass. When applied in the context of QCD, the nucleons were later replaced by (nearly) massless up and down quarks and the model Lagrangian takes the form

$$\mathcal{L}_{\mathrm{NJL}} = \bar{q}(i\gamma^\mu \partial_\mu - m_q)q + G[(\bar{q}q)^2 + (\bar{q}i\gamma_5\vec{\tau}q)^2]. \qquad (11)$$

The interaction between quarks and antiquarks is constructed in a manifestly chirally invariant fashion such that $\mathcal{L}_{\mathrm{NJL}}$ is invariant under left-right transformations of the quark fields in the limit $m_q \to 0$ (chiral limit).[14] Gluons do not appear explicitly but are subsumed in an effective short-range interaction of strength G between the quarks. For sufficiently large G, chiral symmetry is dynamically broken in the ground state through the condensation of quark-antiquark pairs, i.e., the vacuum expectation value $\langle \bar{q}q \rangle$ becomes nonvanishing. This is an effect that cannot be produced by perturbation theory. As a consequence, a gap in the quark energy spectrum occurs. This is in direct analogy to metallic superconductivity in which, according to the Bardeen-Cooper-Schrieffer (BCS) (Bardeen *et al.*, 1957) theory, pairs of electrons interact via the exchange of lattice phonons and condense.

In a quantum field theory the elementary excitations of the vacuum are interpreted as particles. In the original NJL model the energy gap determines the mass of the nucleon. It is finite even in the absence of a "bare mass." Thus mass generation becomes intimately linked to the nontrivial structure of the vacuum. In particle physics this idea of Nambu was new. Replacing nucleons by quarks, the (nearly massless) quarks acquire a con-

---

[11]Here it has been assumed that only up and down flavors contribute significantly to the quark pressure.

[12]At the same time massless left- and right-handed fermions transform into each other under a parity transformation.

[13]The QED Lagrangian (3) is also chirally symmetric in the limit of vanishing m_e. On atomic scales this symmetry is, however, badly broken.

[14]Since two quark flavors are involved, the transformation group is the direct product of the "isospin group" SU(2), acting on left- and right-handed quarks, i.e., SU(2)$_L \times$ SU(2)$_R$.
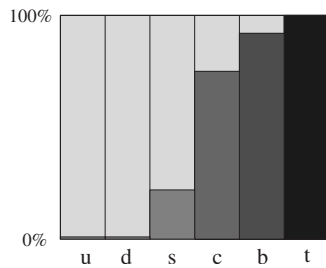
FIG. 3. Fraction of the effective quark mass generated dynamically (light gray) as compared to that from the Higgs mechanism in the electroweak sector of the standard model (dark gray).
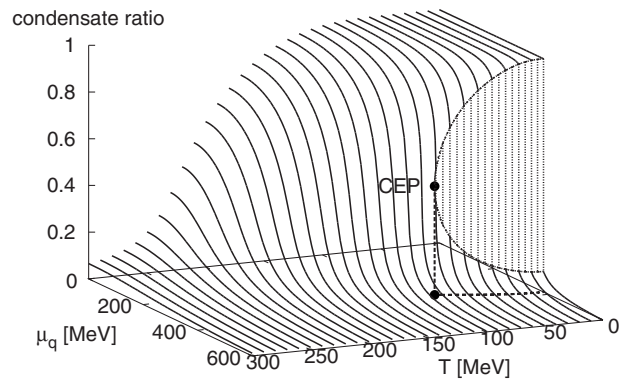

FIG. 4. Evolution of the chiral-condensate ratio $\langle \bar{q}q \rangle_{T,\mu_q}/\langle \bar{q}q \rangle$ plotted on the vertical axis with temperature and quark chemical potential as predicted by the NJL model. The region of first-order transitions, where the condensate ratio jumps discontinuously, is clearly visible. The location of the critical end point (CEP) and its projection onto the (T, μ_q) plane is also indicated. From Heckmann, 2007.

stituent mass M_q of around 300–400 MeV. Since a nucleon consists essentially of three constituent quarks, its mass scale is thus explained. It turns out that dynamical mass generation is not only a feature of the NJL model but actually happens in QCD itself as can be shown from *ab initio* solutions of QCD at large coupling. Figure 3 summarizes the current status of dynamical and Higgs contributions to the effective quark masses (Fischer, 2006) using the Schwinger-Dyson formalism.

As can be seen, the dynamical contribution becomes less important the larger the bare or Higgs mass of the quark. While the heaviest top-quark mass is entirely generated by the Higgs mechanism, for up and down quarks close to 99% of their mass is dynamical. It is, thus, fair to say that almost all of the mass in the visible Universe is created through the nonperturbative structure of the QCD vacuum.

In QCD, mesons emerge as bound states of quark-antiquark pairs with constituent mass. Because of spontaneous chiral symmetry breaking there appears, however, a peculiarity that is known from condensed matter physics and was first noted by J. Goldstone (1961). For vanishing (bare) quark mass there must be a massless excitation of the vacuum, known as the "Goldstone mode." Such highly collective modes occur, e.g., in spin systems. The ferromagnetic ground state has a spontaneous alignment of all spins. A spin wave of infinite wavelength ($\lambda \rightarrow \infty, k \rightarrow 0$) corresponds to a simultaneous rotation of all spins, which costs no energy.[15] In strong interaction physics with two flavors, this mode is identified with the pion. The fact that pions are not exactly massless is related to the finite bare mass of the up and down quarks. Nevertheless, the pion mass with ~140 MeV is significantly smaller than that of the ρ or the ω meson (~ 800 MeV $\sim 2M_q$).

In the 1980s and 1990s the NJL model was used extensively in theoretical studies of the phase diagram. Since it incorporates spontaneous symmetry breaking and the ensuing mass generation, one can address questions of chiral symmetry restoration with increasing T and μ_q and the corresponding medium modifications of

hadron masses. The quark-antiquark condensate $\langle \bar{q}q \rangle$ serves as an order parameter for chiral symmetry breaking, analogous to the spontaneous magnetization in a spin system. Similar to the Curie-Weiss transition, the order parameter vanishes at a critical temperature T_c in the chiral limit. This is the point where chiral symmetry is restored and the quarks become massless.[16] Figure 4 displays a prediction for the evolution of the chiral condensate with temperature and quark-chemical potential for physical up and down quark masses obtained in mean-field theory.

While along the T axis there is a continuous decrease, indicating a smooth restoration of chiral symmetry, one observes along the μ_q axis a first-order phase transition in which the condensate develops a discontinuity. With increasing T this transition becomes weaker and ends in a critical end point (CEP) where the transition is second order. This is analogous to the liquid-gas transition in water (Fig. 1).

III. RESULTS FROM LATTICE QCD

As described in the previous section one may predict, using the schematic bag model and the NJL model (both focusing on different aspects of the strong interaction), that upon heating and compression strongly interacting matter undergoes a relatively abrupt transition from the hadronic phase to the QGP. The relevant scales for this to happen are in the realm of very strong coupling $\alpha_s \sim 1$. Hence, as for the description of any phase transition, the application of perturbative methods, which are very successful for QCD processes at high energies, must fail. The only known way to solve the QCD equations from first principles in the region of strong coupling is to discretize the QCD Lagrangian density on a discrete Euclidean space-time lattice. Here one makes

---

[15]Spin waves obey the dispersion relation $E \propto k^2$. In Lorentz-invariant theories $E \propto k$ for massless particles.

[16]In the NJL model one finds $M_q = m_q - 2G\langle \bar{q}q \rangle$.

use of the formal analogy between Feynman's path-integral formulation of a quantum field theory in imaginary time $\tau = it$ and the statistical mechanics of a system with temperature $T = 1/\tau$.[17] With this method of lattice QCD the partition function of the grand canonical ensemble in the path integral formulation

$$\mathcal{Z}(V,T,\mu_q) = \int \mathcal{D}[A,q]\exp\left(-\int_0^{1/T} d\tau \int_V d^3x\right.$$
$$\left.\times(\mathcal{L}_{\mathrm{QCD}}^E - i\mu_q q^\dagger q)\right) \qquad (12)$$

can be evaluated stochastically via Monte Carlo sampling of field configurations, at least at vanishing μ_q. In Eq. (12) $\mathcal{L}_{\mathrm{QCD}}^E$ denotes the Euclidean version of the QCD Lagrangian density (6).

From the partition function, the thermodynamic state functions such as energy density and pressure can be determined as

$$\varepsilon \equiv \frac{E}{V} = \frac{T^2}{V}\left(\frac{\partial \ln \mathcal{Z}}{\partial T}\right)_{V,\mu_q} + \mu_q\frac{N}{V}; \quad p = T\left(\frac{\partial \ln \mathcal{Z}}{\partial V}\right)_{V,\mu_q}$$
$$(13)$$

in the thermodynamic limit $V, N \to \infty$; $N/V = \mathrm{const}$. At least for matter with an equal number of baryons and antibaryons, i.e., for vanishing baryochemical potential $\mu_b = 3\mu_q$, one obtains in this way quantitative predictions for the temperature dependence of thermodynamic quantities (Karsch, 2002). Results are displayed in Fig. 5.

To emphasize deviations from the Stefan-Boltzmann behavior expected for a free quark-gluon gas one typically shows the reduced energy density ε/T^4 and pressure p/T^4. Near a critical temperature of $T_c = 175$ MeV the reduced energy density shows a rapid ($\Delta T/T_c \lesssim 0.1$) variation, which signals the transition from hadronic matter to the QGP. The critical energy density $\epsilon(T_c)$ is 700 ± 300 MeV/fm^3 which is roughly five times higher than the energy density in the center of a heavy nucleus like ^{208}Pb. At the same time the chiral condensate $\langle \bar{q}q \rangle = \partial p/\partial m_q$ diminishes rapidly near T_c, signaling the restoration of broken chiral symmetry. As indicated in Fig. 5 a systematic discrepancy of about 15% between the calculated energy density (and pressure) and the free gas Stefan-Boltzmann limit is observed for $T > 2T_c$. Although this is roughly consistent with the first-order correction from perturbation theory, the perturbation series is poorly convergent and resummation techniques have to be employed (Blaizot *et al.*, 2006) for a quantitative understanding of the high-temperature EoS.

These *ab initio* numerical findings support the simple

---

[17]The connection between a quantum system governed by the Hamiltonian H and its statistical description is made by considering the transition amplitude $\langle f|e^{-itH}|i\rangle$ from an initial state i to the final state f. Comparing this to the partition function $\mathcal{Z} = \mathrm{Tr}(e^{-\beta H})$ ($\beta = 1/T$) one sees that $\mathcal{Z}$ can be obtained from the transition amplitude by the replacement $it = \beta$, setting $i = f = n$ and summing over n.
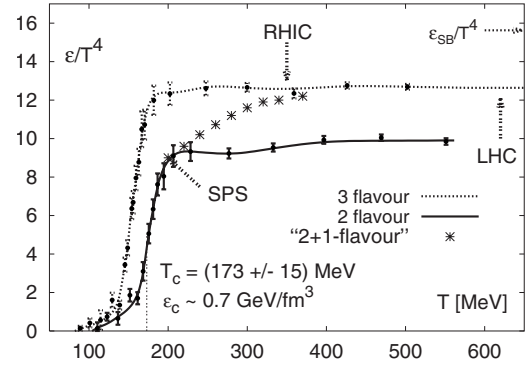

FIG. 5. The temperature dependence of the energy density from numerical solutions of the QCD equations on a discrete (Euclidean) space-time lattice. The full line and dotted line denote results with two quark flavors (up and down) and three flavors (up, down, and strange) of equal mass. The crosses indicate the realistic case for which the strange quark mass is roughly 150 MeV larger than the up and down masses. The arrows indicate the corresponding energy densities and temperatures reached in current (SPS, RHIC) and future (LHC) heavy-ion experiments (see Sec. IV). For details see text. From Karsch, 2002.

model results for the existence of a QGP transition discussed above. In this connection it should be mentioned, however, that most lattice calculations still have to use unrealistically large values for the light quark masses and rather small space-time volumes. With anticipated high-performance computers in the range of hundreds of Teraflop/s, these calculations will be improved in the near future. Ultimately they will also provide definite answers concerning the nature of the transition. Among others, this is of importance for primordial nucleosynthesis, i.e., the formation of light elements, such as deuterium, helium, and lithium. In a strongly first-order quark-hadron transition, bubbles form due to statistical fluctuations, leading to significant spatial inhomogeneities. These would influence the local proton-to-neutron ratios, providing inhomogeneous initial conditions for nucleosynthesis (Applegate *et al.*, 1988; Thomas *et al.*, 1993; Schwarz, 1998; Boyanovsky *et al.*, 2006). Other consequences would be the generation of magnetic fields, gravitational waves, and the enhanced probability of black-hole formation (Boyanovsky *et al.*, 2006).

At present, indications are that for $\mu_q = 0$, relevant for the early Universe, the transition is a "crossover," i.e., not a true phase transition in the thermodynamic sense (Aoki, Endrodi, *et al.*, 2006). Near T_c the state functions change smoothly but rapidly, as discussed above. For most of the experimental observables to be discussed below this subtlety is, however, of minor relevance. A crossover would wash out large spatial fluctuations and hence rule out inhomogeneous cosmic scenarios. Recent studies (Aoki, Fodor, *et al.*, 2006; Cheng *et al.*, 2006) indicate that the exact value of the transition temperature is still poorly known. In fact, these investigations have yielded values for T_c in the range 150–190 MeV. This is in part due to difficulties with the necessary extrapola-

tion to the thermodynamic (infinite volume) limit and in part due to the general difficulty in providing an absolute scale for the lattice calculations. Progress in this area is expected with simulations on much larger lattices at the next generation computer facilities.

While at $\mu_q=0$ the lattice results are relatively precise, the *ab initio* evaluation of the phase boundary in the (T, μ_q) plane (Fig. 4) poses major numerical difficulties. This is basically related to the Fermi-Dirac statistics of the quarks and is known in many-body physics as the "fermion-sign problem." For the integral (12) this implies that the integrand becomes an oscillatory function and, hence, Monte Carlo sampling methods cease to work. Only recently new methods have been developed (de Forcrand and Philipsen, 2002; Fodor and Katz, 2002; Allton *et al.*, 2003; Philipsen, 2006) to go into the region of finite μ_q.

What can be expected? Considering the phase boundary as a line of (nearly) constant energy density, the bag model (Braun-Munzinger and Stachel, 1996) predicts that the critical temperature decreases with increasing μ_q. By construction the bag model describes a first-order phase transition for all chemical potentials. For large values of μ_q and low temperatures there are indications from various QCD-inspired model studies, chiefly the NJL model (see Fig. 4), that the (chiral) phase transition is indeed first order. On the other hand, the lattice results discussed above seem to indicate that, at very small μ_q, the transition is a crossover. This would imply that there is a critical end point in the phase diagram, where the line of first-order transitions ends in a second-order transition (as in the liquid-gas transition of water). In analogy to the static magnetic susceptibility $\chi_M = \partial M / \partial H$ in a spin system one can define a "chiral susceptibility" as the derivative of the in-medium chiral condensate $\langle \bar{q}q \rangle_{T, \mu_q}$ with respect to the bare quark mass m_q or equivalently as the second derivative of the pressure, $\chi_m = \partial \langle \bar{q}q \rangle_{T, \mu_q} / \partial m_q = \partial^2 p / \partial m_q^2$. Here the quark mass m_q plays the role of the external magnetic field H. In the Curie-Weiss transition χ_M diverges. The same should happen with χ_m at the CEP. On the other hand, lattice studies and model calculations indicate that the quark number susceptibility $\chi_n = \partial n_q / \partial \mu_q = \partial^2 p / \partial \mu_q^2$ also diverges. This implies that in the vicinity of the CEP matter becomes easy to compress since the isothermal compressibility is given by $\kappa_T = \chi_n / n_q^2$. It is conjectured that the critical behavior of strongly interacting matter lies in the same universality class as the liquid-gas transition of water (Stephanov, 2004). The experimental identification of a CEP and its location in the (T, μ_q) plane would be a major milestone in the study of the phase diagram. Although very difficult, there are several theoretical as well as experimental efforts underway (Proceedings of Science, 2006) to identify signals for such a point. For a recent critical discussion concerning the existence of a CEP in the QCD phase diagram see Philipsen (2007).

IV. EXPERIMENTS WITH HEAVY IONS

The phase diagram of strongly interacting matter can be accessed experimentally in nucleus-nucleus collisions at ultrarelativistic energy, i.e., energies per nucleon in the center of mass (c.m.) frame that significantly exceed the rest mass of a nucleon in the colliding nuclei. After first intensive experimental programs at the Brookhaven Alternating Gradient Synchrotron (AGS) and the CERN Super Proton Synchrotron (SPS), the effort is at present concentrated at the Relativistic Heavy-Ion Collider (RHIC) at Brookhaven. A new era of experimental quark matter research will begin in 2009 with the start of the experimental program at the CERN Large Hadron Collider (LHC). Here we will not attempt to give an overview of the experimental status in this field (for recent reviews see Gyulassy and McLerran, 2005 and Braun-Munzinger and Stachel, 2007) but concentrate on a few areas which in our view have direct bearing on the phase diagram. Before doing so we will, however, briefly sketch two of the key results from RHIC, which have led to the discovery that quark-gluon matter in the vicinity of the phase boundary behaves more like an ideal liquid rather than a weakly interacting plasma.

A. Opaque fireballs and the ideal liquid scenario

At RHIC, Au-Au collisions are investigated at c.m. energies of 200 GeV per nucleon pair. In such collisions a hot fireball is created, which subsequently cools and expands until it thermally freezes out[18] and free-streaming hadrons reach the detector. The spectroscopy of these hadrons (and the much rarer photons, electrons, and muons) allow conclusions about the state of the matter inside the fireball, such as its temperature and density. The four experiments at RHIC have recently summarized their results (Adams *et al.*, 2005b; Adcox *et al.*, 2005; Arsene *et al.*, 2005; Back *et al.*, 2005) For a complete overview see also the proceedings of the three recent quark matter conferences (Proc. Quark-Matter 2005 Conference, 2006; Proc. Quark-Matter 2006 Conference, 2007; Proc. Quark-Matter 2008 Conference, 2008).

The produced fireball has such a high density and temperature that apparently all partons (quarks and gluons) reach equilibrium very rapidly (over a time scale of less than 1 fm/c). Initially, the collision zone is highly anisotropic with an almondlike shape, at least for collisions with not too small impact parameter. The situation is schematically described in Fig. 6. In this equilibrated anisotropic volume large pressure gradients exist, which determine and drive the hydrodynamic evolution of the fireball. Indeed, early observations at RHIC confirmed that the data on the flow pattern of the matter follow

---

[18] A thermal freeze-out is defined as the point in temperature where the density of particles with elastic cross section σ becomes small enough so that the mean free path $\lambda = 1/n\sigma$ is larger than the system size.
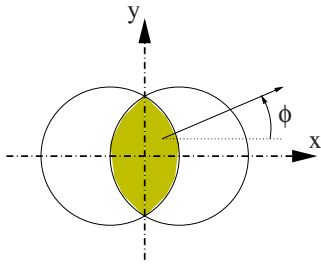
FIG. 6. (Color online) Geometry of the fireball in the plane perpendicular to the beam direction in a nucleus-nucleus collision with large impact parameter.

closely the predictions (Huovinen *et al.*, 2001; Teaney *et al.*, 2002; Kolb and Heinz, 2004) based on the laws of ideal relativistic hydrodynamics. By Fourier analysis of the distribution in azimuthal angle Φ (see Fig. 6) of the momenta of produced particles, the Fourier coefficient $v_2 = \langle \cos(2\Phi) \rangle$ can be determined as a function of the particles transverse momentum p_t. These distributions can be used to determine the anisotropy of the fireball's shape and are compared, in Fig. 7 for various particle species, to the predictions from hydrodynamical calculations. The observed close agreement between data and predictions, in particular concerning the mass ordering of the flow coefficients, implies that the fireball flows collectively like a liquid with negligible shear viscosity η. Similar phenomena were also observed in ultracold atomic gases of fermions in the limit of very large scattering lengths, where it was possible, by measuring η through analysis of the damping rates of breathing modes, to establish that the system is in a strongly coupled state (O'Hara *et al.*, 2002).
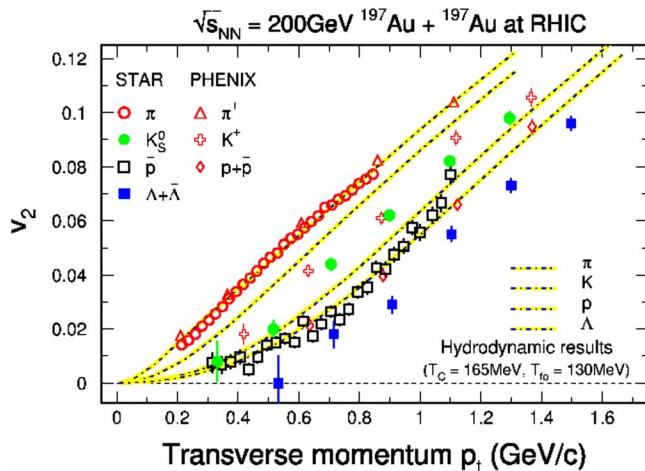

FIG. 7. (Color online) The Fourier coefficient v_2 for pions, kaons, protons, and Λ baryons (with masses of 140, 495, 940, and 1115 MeV, respectively) emitted with transverse momentum p_t in semicentral Au-Au collisions at RHIC. The data are from the STAR Collaboration (Adams *et al.*, 2005a). The lines correspond to predictions (Huovinen *et al.*, 2001) from hydrodynamical calculations with an equation of state based on weakly interacting quarks and gluons.
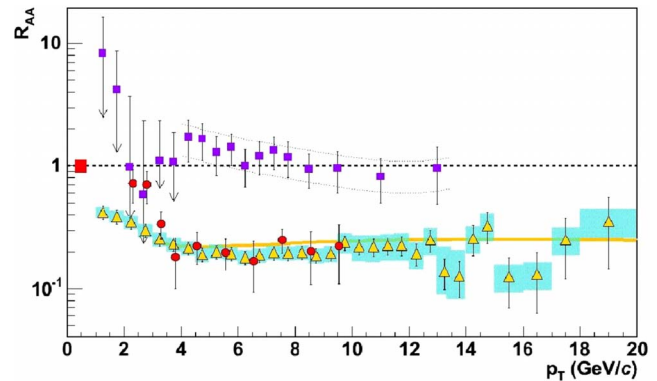

FIG. 8. (Color online) Results from the PHENIX Collaboration (Akiba, 2006; Adler *et al.*, 2007) for the p_t dependence of the suppression factor R_{AA}. The suppression visible in the data for π^0 and η mesons provides evidence for the presence of a dense medium scattering partons at high p_t and degrading their momenta. Photons which undergo only electromagnetic interactions do not exhibit the effect. The bands provide an estimate of systematic uncertainties. The solid line represents a theoretical spectrum (Vitev, 2006) calculated under the assumption that the initially high p_t parton loses energy by gluon radiation in the dense gluon gas inside the fireball.

This liquidlike fireball is dense enough that even quarks and gluons of high momentum (jets) cannot leave without strong rescattering in the medium. This "jet quenching" manifests itself in a strong suppression (by about a factor of 5) of hadrons with large momenta transverse to the beam axis compared to expectations from a superposition of binary nucleon-nucleon collisions. The interpretation is that a parton which eventually turns into a hadron must suffer a large energy loss while traversing the hot and dense collision zone. To make matters quantitative one defines the suppression factor R_{AA} as the ratio of the number of entries at a given transverse momentum p_t in Au-Au collisions to that in proton-proton collisions, scaled to the Au-Au system by the number of binary nucleon-nucleon collisions such that, in the absence of parton energy loss, $R_{AA} = 1$. Corresponding data are presented in Fig. 8. The strong suppression observed by PHENIX and, in fact, by all RHIC collaborations (Adams *et al.*, 2005b; Adcox *et al.*, 2005; Arsene *et al.*, 2005; Back *et al.*, 2005) demonstrates the opaqueness of the fireball even for high momentum partons, while photons, which do not participate in strong interactions, can leave the fireball unscathed. Theoretical analysis of these data (Gyulassy and McLerran, 2005; Vitev, 2006) provides evidence, albeit indirectly, for energy densities exceeding 10 GeV/fm^3 in the center of the fireball. Very interestingly, the fireball is apparently opaque enough to strongly affect the spectra of heavy (c and b) quarks (Adler *et al.*, 2006b; Abelev *et al.*, 2007). This was not expected in view of the arguments put forward by Dokshitzer and Kharzeev (2001). Although the mechanism for heavy-quark energy loss is not well understood, the data provide evidence for their scattering and thermalization in the fireball. This will become important for the

later discussion about quarkonia. There is even evidence (Adler *et al.*, 2006a) for the presence of Mach conelike shock waves (Casalderrey-Solana *et al.*, 2005; Stoecker, 2005), and Teaney caused by supersonic partons traversing the QGP. Apparently both elastic parton-parton collisions as well as gluon radiation contribute to the energy loss but it is fair to say that the details of this mechanism are currently not well understood. The situation has been summarized by Gyulassy and McLerran (2005).

With the start of the nucleus-nucleus collision program at the LHC in the Fall of 2009 the current understanding of jet quenching and of the ideal-fluid behavior of the hot fireball will be subjected to decisive tests. At the much higher LHC energy, initial temperatures close to 1 GeV can be reached and the fireball is probed with partons in the 100 GeV range. It will be exciting to see how the currently developed concepts will evolve with the data from this new era.

B. Hadrochemistry

In ideal hydrodynamics no entropy is generated during the expansion and cooling of the fireball, i.e., the system evolves through the phase diagram along isentropes, starting in the QGP phase. This can be experimentally verified through the production of a variety of mesons and baryons. The analysis of particle production data at AGS, SPS and RHIC energies has clearly demonstrated (Becattini *et al.*, 2004, 2006; Braun-Munzinger, Redlich, and Stachel, 2004; Andronic *et al.*, 2006) that the measurements can be understood to a high accuracy by a statistical ansatz in which all hadrons are produced from a thermally and chemically equilibrated state. This hadrochemical equilibrium is achieved during or very shortly after the phase transition and leads to abundances of the measured hadron species that can be described by Bose-Einstein or Fermi-Dirac distributions

$$n_j = \frac{g_j}{2\pi^2} \int_0^\infty p^2 dp (\exp\{[E_j(p) - \mu_j]/T\} \pm 1)^{-1} \quad (14)$$

of an ideal relativistic quantum gas. Here $E_j^2 = M_j^2 + \vec{p}_j^2$ is the relativistic energy-momentum relation of free hadrons of mass M_j, μ_j is the chemical potential of this species, and g_j counts the number of degrees of freedom, such as spin and charge state of a given hadron. The results of such an analysis for the measured abundances in central Au-Au collisions at a c.m. energy per nucleon pair of $\sqrt{s_{NN}} = 130$ GeV at RHIC are shown in Fig. 9.

Such calculations give, for each beam energy, a set of two thermodynamic variables, namely, temperature T and baryochemical potential μ_b at the point of hadroproduction, i.e., at chemical freeze-out.[19] This is consistent with the assumption that all particles were pro-
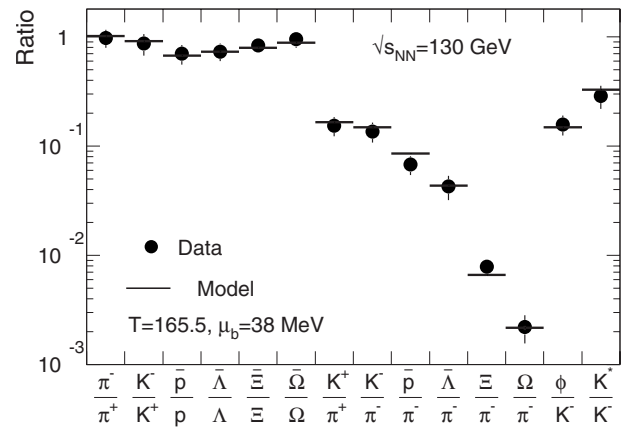

FIG. 9. Ratios of particle multiplicities in central Au-Au collisions at RHIC energies in comparison with a fit from a statistical model of thermally and chemically equilibrated hadrons. From Andronic *et al.*, 2006.

duced at the same instant, i.e., at the same temperature and chemical potential. Such analyses also provide a striking confirmation for the concept of a limiting temperature T_H discussed above (Hagedorn 1965), as shown in Fig. 10.

The significance of these results is further appreciated by entering the (T, μ_b) values of fixed beam energy into the phase diagram (Fig. 11), establishing the "chemical
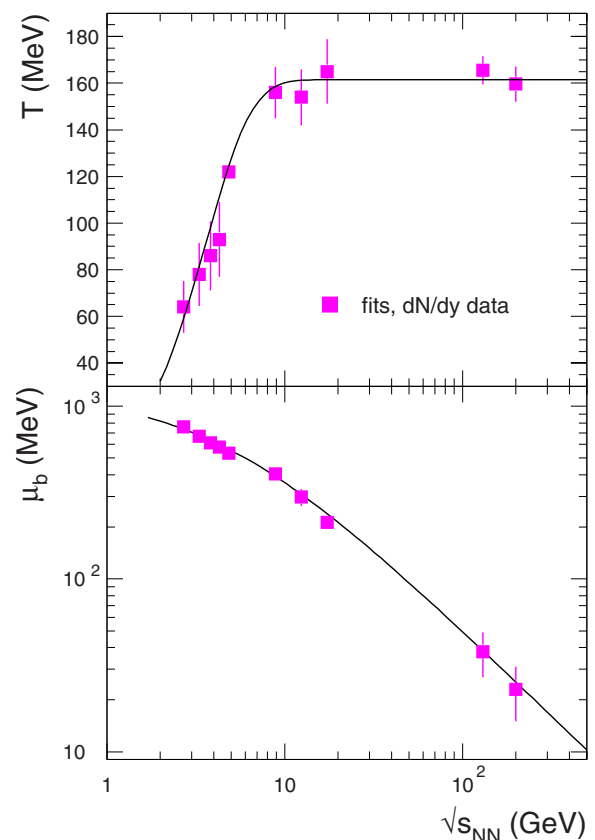

FIG. 10. (Color online) Energy dependence of thermal parameters T and μ_b from a statistical analysis (Andronic *et al.*, 2006) of hadrons produced in central nucleus-nucleus collisions.

---

[19]Chemical freeze-out occurs when inelastic collisions between particles cease such that the abundance ratios do not change anymore.
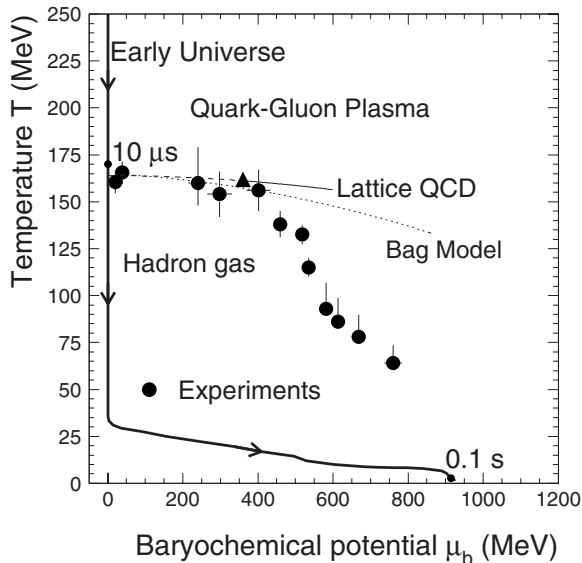
FIG. 11. The QCD phase diagram and data from a chemical freeze-out analysis in nucleus-nucleus collisions at various beam energies. The data points closest to the T axis are from the highest collision energies. For the other entries see text.

freeze-out curve" (Braun-Munzinger and Stachel, 1996, 1998; Braun-Munzinger *et al.*, 1996). It was noted early on (Cleymans and Redlich, 1998) that this curve can be understood phenomenologically by assuming that the freeze-out takes place at a constant energy per particle of about 1 GeV.

In Fig. 11 the experimental points for chemical freeze-out are compared with the phase boundary from lattice QCD (Fodor and Katz, 2004) and from the bag model (Braun-Munzinger and Stachel, 1996). For illustration a recent theoretical prediction for the possible location of the CEP (Fodor and Katz, 2004) is also shown (triangle) as well as the trajectory that the early Universe has taken in the standard big bang model.[20] It is interesting to note that for $\mu_b < 250$ MeV the experimental freeze-out points are close to the calculated phase boundary of (Fodor and Katz, 2004). This does not come as a surprise. On the contrary, there are good arguments that the phase transition itself is responsible for the equilibration of all hadron species. In a recent analysis (Braun-Munzinger, Stachel, and Wetterich, 2004) it was shown that because of the strongly increasing particle density near the phase boundary multiparticle collisions dominantly contribute to the particle production. This leads to a rapid equilibration ($\tau < 1$ fm) of Λ baryons

and even of baryons with multiple strangeness content (Ξ, Ω baryons) compared to the typical expansion time of the fireball of several fm. It also explains naturally why all particles freeze out in a relatively short time at nearly constant temperature. Similar conclusions, although based on different arguments, can be found in works by Heinz (1998); Stock (1999); and Heinz and Kestin (2006). The general result from these findings is that, at least at small μ_b, the temperatures extracted from the chemical analysis are closely linked to T_c obtained from the calculated QCD phase boundary. Thus, for the first time, a fundamental parameter of the phase diagram, namely, the critical temperature T_c at small μ_b, has been confronted with experiment and the agreement is very good.[21]

For larger values of μ_b the measured freeze-out points deviate from the predictions of lattice QCD (Fig. 11). At present it is hotly debated whether this deviation indicates the existence of a highly compressed hadronic phase between the QCD phase boundary and the chemical freeze-out line, or whether the calculation of the phase boundary at large μ_b will be modified by significant corrections from realistic quark masses and larger space-time lattices. Important new insight is expected from measurements with the "Compressed Baryonic Matter" (CBM) experiment planned at the future "Facility for Antiproton and Ion Research" (FAIR) at GSI in Darmstadt, as well as from improved lattice simulations.

The thermalization described above implies that equilibrated matter is produced in high-energy collisions between nuclei. In e^+e^- and hadron-hadron collisions, such an equilibration, in particular in the strangeness sector, is not observed (Braun-Munzinger, Redlich, and Stachel, 2004) although thermal features are observed in the yields of produced particles (Becattini, 1996; Becattini and Heinz, 1997). For very recent discussions of differences and similarities between e^+e^- and nucleus-nucleus collisions see Becattini *et al.* (2008) and Andronic *et al.* (2009).

For the high-energy domain accessible with Pb ions at the LHC the scenario described implies essentially small changes in hadron production (apart from an overall yield factor due to the much larger volume). Any deviation would be a major surprise and would likely indicate new physics. For speculations in this direction see Rafelski and Letessier (2008).

---

[20]This trajectory is evaluated (Braun-Munzinger and Wambach, 2006) by assuming that the early Universe expanded isentropically under the conditions of charge neutrality and net lepton—net baryon number conservation and that the entropy per baryon is fixed using the known baryon to photon ratio; see also Fromerth and Rafelski (2002) and Kampfer *et al.* (2007). Furthermore, the evolution proceeds in full chemical equilibrium among hadrons and leptons until the neutrinos freeze out at a time of about $t=1$ s.

---

[21]We neglect the above discussed uncertainty in T_c obtained from recent lattice calculations (Aoki, Fodor, *et al.*, 2006; Cheng *et al.*, 2006). It should be pointed out, however, that a value of $T_c = 190$ MeV is inconsistent with the scenario discussed here and would probably imply the presence of an ultradense hadronic phase between chemical freeze-out and the phase boundary. There is currently no indication of such a phase from experiment.

C. Medium modifications of vector mesons

As the spontaneously broken chiral symmetry of the strong interaction gets restored at high temperatures and large chemical potentials, the quarks loose their constituent mass and only the bare masses generated in the Higgs sector of the standard model are left. As seen from Fig. 3 this effect is most dramatic for up and down quarks and to a somewhat lesser extent also for strange quarks. Most naively the mass of a hadron is a multiple of the constituent quark mass M_q (for baryons $M_b \sim 3M_q$ and for mesons $M_m \sim 2M_q$), and one would therefore expect that all hadron masses consisting of light u, d, and s quarks should decrease significantly near the phase boundary (Brown, 1988). More general arguments along these lines led to the conjecture of a general scaling law in which (nearly) all light hadrons consisting of u and d quarks change with some power of the chiral condensate ratio (Brown and Rho, 1991) "Brown-Rho scaling"[22]

$$M_h \propto (\langle \bar{q}q \rangle_{T,\mu_b}/\langle \bar{q}q \rangle)^{\alpha}. \tag{15}$$

Another obvious source of medium modifications of hadrons is the increased collision rate in a hot and dense medium. As a consequence, many new decay channels open, resulting in large widths. Finally, based on chiral symmetry alone and its spontaneous breaking in the vacuum, it can be argued that the spectral properties of hadrons with opposite parity become more and more similar as the chiral phase transition is approached.

Since possible modifications of hadron properties (masses, decay modes) occur in the hot and dense phase of a heavy-ion collision, one needs an experimental probe that is sensitive to this state of the matter. More than 30 years ago it was suggested (Feinberg, 1976; Shuryak, 1978) that real or virtual[23] photons are ideal since they interact only electromagnetically with the surrounding matter and hence leave the reaction zone almost undisturbed. Even at the highest temperatures and compression reached in relativistic heavy-ion collisions the mean free path of photons is typically 10^2–10^4 fm, which is much larger than the size of the fireball.

Both longitudinal and transverse photon polarizations contribute to the di-lepton rate, while real photons can only be transversely polarized. According to Fermi's golden rule the production cross section is directly related to the (auto)correlation function $\langle j_{elm}^{\mu} j_{elm}^{\mu} \rangle$ of the electromagnetic current, which involves the charge carriers of the system. Taking quarks as fundamental constituents of strongly interacting matter, j_{elm} is given by

$$j_{elm}^{\mu} = \sum_{i=u,d,s} e_i \bar{q}_i \gamma^{\mu} q_i = \tfrac{2}{3} \bar{u} \gamma^{\mu} u - \tfrac{1}{3} \bar{d} \gamma^{\mu} d - \tfrac{1}{3} \bar{s} \gamma^{\mu} s. \tag{16}$$

(For the measurements discussed below only the three light quark flavors are relevant.) It is well established by precision measurements that the $e^+ e^-$ annihilation cross section below c.m. energies of $\simeq 1.2$ GeV is essentially saturated by the light vector mesons ρ, ω, ϕ with the ρ meson giving the largest contribution ($\sim 9:1:2$). Therefore, the in-medium modification of the ρ meson in di-lepton production in heavy-ion collisions is of particular interest. Also the large ($\Gamma = 150$ MeV) width implies that the ρ meson decays and is regenerated several times during the lifetime of the fireball: the resulting di-leptons then carry information about its interior.

In physical terms the di-lepton signal is, therefore, dominantly due to pion annihilation $\pi^+ \pi^- \to \rho \to e^+ e^-$ in the hadronic phase or quark annihilation $\bar{q}q \to e^+ e^-$ in the partonic phase. If we assume that the fireball formed in an ultrarelativistic nucleus-nucleus collision is close to thermal equilibrium then the above formalism leads to di-lepton (photon) spectra after convolution of the relevant transition rates with the hydrodynamic space-time evolution of the system.

Experiments to measure di-lepton production in nuclear collisions have been conducted since the late 1980s starting with data taking at the DLS experiment (Roche *et al.*, 1989; Porter *et al.*, 1997) in Berkeley. For a historical account of lepton pair production measurements in general see Specht (2008). Here we focus on the most recent measurements at ultrarelativistic energies and the current status of their interpretation. To search for nontrivial contributions the data for di-lepton measurements are compared to predictions for yields resulting from the electromagnetic decay of hadrons at chemical freeze-out. The hadron production rate is either directly measured or inferred from statistical model calculations discussed above (Braun-Munzinger, Redlich, and Stachel, 2004). The resulting yields are called "hadronic cocktail" as they result from the standard known mixture of unmodified hadronic resonances.

Pioneering results on the production of $e^+ e^-$-pairs came from the DLS (Porter *et al.*, 1997), HELIOS (Angelis *et al.*, 1998), and CERES (Agakichiev *et al.*, 1995, 2005; Agakishiev *et al.*, 1998) collaborations: the main and dramatic outcome of these experiments was that all central nucleus-nucleus collision measurements exhibited a yield that is strongly enhanced compared to predictions for cocktail decays in the invariant mass range $0.2 < m_{e^+e^-} < 1.1$ GeV. Theoretical analysis of the excess observed in the CERES data (Rapp and Wambach, 2000) indicated that the enhancement is due to a strong increase of the ρ-meson width in the hot and dense medium formed in the collision. The excess disappears for more peripheral collisions (Agakichiev *et al.*, 2005) (which exhibit features more like nucleon-nucleon collisions) but for SPS energies the beam energy dependence of the observed effect is small (Adamova *et al.*, 2003). A satisfactory explanation of the excess observed by DLS at much lower energies remained missing.

---

[22]The pion is special because of its "Goldstone character" and therefore its mass should remain largely unaffected.

[23]Virtual timelike photons correspond to the process of di-lepton ($e^+ e^-$ or $\mu^+ \mu^-$) pair production or annihilation.
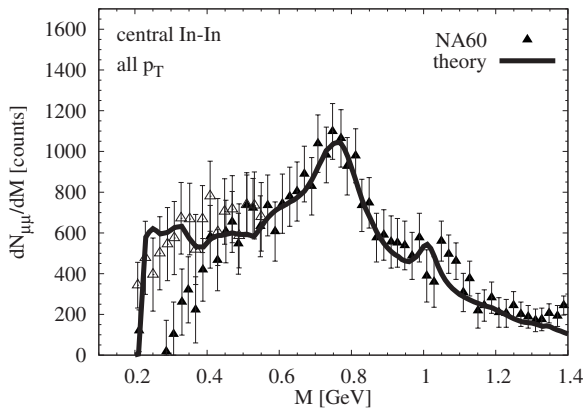
FIG. 12. The NA60 low mass spectrum after subtraction of "cocktail" decay processes after thermal freeze-out compared with the theoretical predictions from van Hees and Rapp (2006, 2008). The open data points exhibit the size of the correction resulting from a decrease in the η yield by 10%. From Arnaldi *et al.*, 2006.
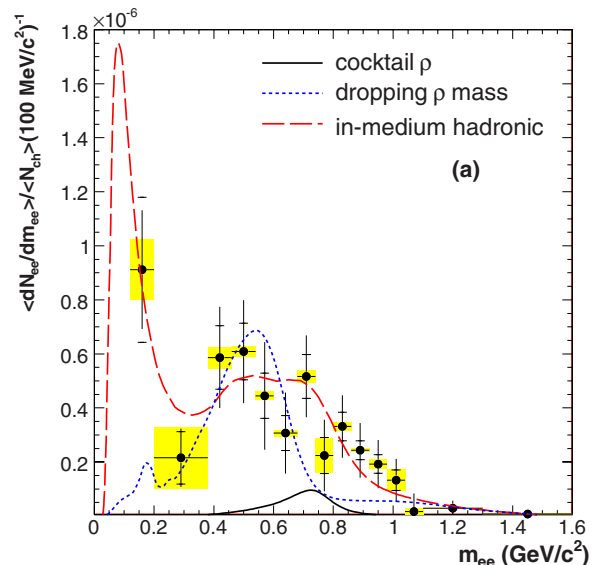

FIG. 13. (Color online) The CERES low mass spectrum compared with theoretical predictions from the "dropping mass" scenario (Brown and Rho, 1991) and hadronic many-body theory (Rapp and Wambach, 2000; van Hees and Rapp, 2007, 2008).

Dramatic progress was recently achieved by the NA60 Collaboration which, for a collision system of intermediate mass (In+In), provided data (Arnaldi *et al.*, 2006) in the di-muon channel with very good statistics and improved mass resolution compared to previous measurements. The quality of the data is such that the di-lepton yield resulting from final state hadron decays, i.e., the cocktail yield, can be subtracted from the measured di-lepton spectra. The resulting subtracted spectrum is compared, in Fig. 12, with predictions that take into account all collision processes of the ρ meson with the surrounding particles in the fireball (van Hees and Rapp, 2006, 2008).

Note that the data are not acceptance corrected, implying that the calculations have to be filtered appropriately for a meaningful comparison (Arnaldi *et al.*, 2006; Specht, 2007).

In such many-body calculations, the spectral function of the ρ meson is considerably broadened in the hot and dense medium compared to the line shape of the ρ meson in vacuum. The strong broadening is dominantly due to interactions of ρ mesons with baryons (and antibaryons) in the dense fireball near the phase boundary. This is indeed observed in the NA60 data, as is demonstrated by the quantitative agreement between data and calculations. Note that there is no evidence for a possible downward shift of the ρ mass, as had been predicted early on (Brown and Rho, 1991) based on a scaling relation (15) between the ρ mass and the in-medium quark condensate.

The CERES Collaboration has recently presented (Adamova *et al.*, 2008) their absolutely normalized data on low-mass e^+e^--pair production in central Pb-Au collisions at SPS energy, taken with the upgraded CERES apparatus. Again, to explicitly display the shape of the in-medium contribution to the di-lepton mass spectrum, the cocktail excluding the ρ-meson contribution was subtracted from both the data and theoretical calculations. The result is shown in Fig. 13.

Note that the yield of the "cocktail ρ" is only about 10% of the observed yield near the mass of the vacuum ρ, demonstrating the extremely strong modification of its spectral function in the dense fireball. Calculations based on the many-body approach (Rapp and Wambach, 2000; van Hees and Rapp, 2007, 2008) explain this medium modification quantitatively, while those based on a downward shift of the ρ mass (Brown and Rho, 1991; van Hees and Rapp, 2007a) are at variance with the observations,[24] in accord with the findings of the NA60 Collaboration. Below di-lepton masses of 200 MeV, the CERES data indicate a further strong rise. Such an increase towards the "photon point" ($m_{e^+e^-}=0$) was predicted in a consistent treatment of the in-medium ρ-meson spectral function (Rapp and Wambach, 2000) and its observation lends further support to the underlying theoretical approach.

Two more experiments have released data on di-lepton production in nucleus-nucleus collisions during the past year. The HADES Collaboration presented their first data on C+C collisions at relatively low energy (Agakichiev *et al.*, 2007, 2008), substantially corroborating the measurements of the DLS Collaboration. Currently a significant theoretical effort is underway to understand these observations.

The PHENIX experiment at RHIC has also presented first results on di-lepton production in Au-Au collisions (Afanasiev *et al.*, 2007) at very high energy ($\sqrt{s_{N,N}}=200$ GeV). The results are presented in Fig. 14. In

---

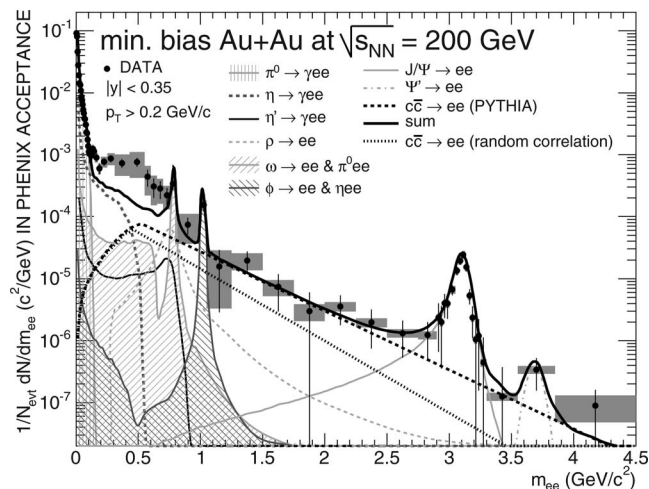[24]See Brown *et al.* (2007) for an updated view on the connection between the ρ mass and the chiral condensate.

FIG. 14. The PHENIX low-mass spectrum for Au-Au collisions at top RHIC. From Afanasiev *et al.*, 2007.

addition to peaks of the vector mesons, one observes a very large enhancement compared to the hadronic cocktail in the di-lepton yield for masses between 200 and 800 MeV. At present, the size of this enhancement is not reproduced within the theoretical approaches described above. Future research will tell whether new physics is visible here or whether these data can also be described within the language of hadronic many-body theories.

Finally we comment on the connection between the medium modification of hadrons and the phase diagram. Already 25 years ago Pisarski (1982) argued that prompt di-lepton production from a hot fireball can be a signal for critical behavior through changes of the mass and width of the ρ meson near the phase boundary. The issue was further investigated by Karsch *et al.* (1993). As discussed above, it is our current understanding that near (or at) the deconfinement phase boundary also chiral symmetry will be restored. The in-medium electromagnetic response, which is dominated by the vector mesons ρ, ω, and ϕ, provides a direct link to chiral symmetry and its restoration near T_c. Restoration of chiral symmetry implies a strong reduction ("melting") of the quark condensate near T_c. Furthermore, at the phase boundary, the vector- and axial-vector correlation functions (see above) corresponding to the ρ meson and its chiral (parity) partner, the a_1 meson, must become identical in the limit of vanishing quark masses (Weinberg, 1967; Kapusta and Shuryak, 1994).

It is an interesting observation (Rapp and Wambach, 1999) that the yield calculated using the hadronic in-medium correlation function near the phase boundary coincides remarkably well with that obtained from lowest-order $q\bar{q}$ annihilation in the QGP, where chiral symmetry is restored. Since a strong increase in the ρ-meson width is seen in the present di-lepton data, it thus seems that the signal for chiral symmetry restoration in the electromagnetic response of hot and dense

matter is a smooth melting[25] of the ρ meson into a featureless quark-antiquark continuum [see also Gallmeister *et al.* (2001) and Kämpfer (2007)]. While this is not a rigorous argument for chiral symmetry restoration by itself, a much stronger case could be made if the modification of the chiral partner a_1 could be measured. On general grounds its spectral distribution has to become degenerate with that of the ρ meson when chiral symmetry is restored. Hence, the a_1 meson also has to melt smoothly into a quark-antiquark continuum. Unfortunately this is hard to check experimentally since the dominant electromagnetic decay of the a_1 meson involves, besides a virtual or real photon, a pion. The latter suffers strong rescattering and absorption in the fireball and hence the early stages of the collision are hard to probe. At low temperatures and densities, however, one can prove that chiral symmetry restoration manifests itself in a mixing of the ρ and a_1 meson through the absorption or emission of a pion from the surrounding medium (Dey *et al.*, 1990).

D. Quarkonia—messengers of deconfinement

In a nucleus-nucleus collision at very high energy heavy quarks, charm or beauty, can be produced rather copiously. For example, the number of charm and anti-charm quark pairs in a Pb-Pb collision at LHC energy might well reach beyond a hundred. Because of the large mass of the charm quarks compared with the typical QCD scale ($\Lambda_{QCD} \approx 200$ MeV, $m_{charm} \approx 1.3$ GeV) there is a separation of time scales between charm quark production and the production of hadrons containing charm quarks (Andronic *et al.*, 2008). The question of medium modifications of such hadrons is then more subtle.

Particles collectively known as "quarkonia" are bound states of charm or beauty quarks and their antiquarks. They play an important role as probes for deconfined matter inside the hot and dense fireball. In their seminal paper Matsui and Satz (1986) argued that the bound state made up of charmed quarks and antiquarks, the J/ψ meson, would be destroyed (or prevented from being formed) by the high density of partons in the QGP. The physics behind this process is similar to Debye screening of the electromagnetic field in an electromagnetic plasma through the presence of movable electric charges. To provide a first estimate, we note that the density of partons (quarks and gluons) in a noninteracting plasma with three massless flavors is $n = 4.2T^3$. At a temperature of 500 MeV, this implies that $n \approx 70/\text{fm}^3$. The mean distance between these color charges scales like $1/n^{1/3} \propto 1/T$ and is about 0.25 fm in the ideal gas

---

[25]Whether the melting occurs only close to the phase boundary or over an extended range of temperatures and densities below the phase boundary is currently an open issue. There are indications, however, that already at chemical freeze-out the baryon density is rather low (Braun-Munzinger and Stachel, 2002).

limit, much less than the spatial extent of the J/ψ meson. Indeed, taking strong interactions among the color charges into account leads to a Debye screening radius $r_D \propto 1/g_s(T)T$, which decreases with increasing temperature. Hence the resulting color screening may destroy the bound state. The suppressed yields of charmonia measured in a high-energy nucleus-nucleus collision (compared to their production in the absence of a QGP) was thus proposed (Matsui and Satz, 1986) as a "smoking gun" signature for the QGP.

Measurements performed during the last decade at the CERN SPS accelerator provided first evidence for such a suppression (Abreu, 2001) in central collisions between heavy nuclei. Little suppression was found in grazing collisions or collisions between very light nuclei, where QGP formation is not expected. The precision data of Abreu (2001) could be described, however, also by considering "normal" absorption of charmonium in the nuclear medium, in conjunction with its possible break up by hadrons produced in the collision (comovers). Such mechanisms could lead to charmonium suppression even in the absence of QGP formation (Gavin and Vogt, 1997; Spieles *et al.*, 1999; Capella *et al.*, 2002) and the interpretation of the SPS data remains inconclusive.

This situation took an interesting turn in 2000, when it was realized that the large number of charm-quark pairs produced in a nuclear collisions at RHIC or LHC energies leads to new mechanisms for charmonium production, either through statistical production at the phase boundary (Braun-Munzinger and Stachel, 2000, 2001) or through coalescence of charm quarks in the plasma (Thews *et al.*, 2001). At low energy, the mean number of charm-quark pairs produced in a collisions is much less than 1, implying that a charmonium state, if at all, is always formed from charm quarks of the one and only pair produced. On the other hand, the number of charm quark pairs at RHIC energies is already much larger than 1 (indirect measurements imply a charm-quark multiplicity of about 10) and the total number of charm quarks in a collision at the LHC is expected to reach values larger than 100. Under such conditions charm quarks from different pairs can combine to form charmonium. Charm-quark recombination works effectively only if the charm quarks can travel a significant distance in the plasma to "meet" with their prospective partner. Under these conditions, charmonium production scales quadratically with the number of charm quark pairs. Thus enhancement, rather than strong suppression, is predicted (Andronic *et al.*, 2007b) for LHC energies. We note that, in the recombination model, it is assumed that charmonia are either not formed before the QGP or that they are completely destroyed by it (complete quenching), so that all charmonium production takes place when the charm quarks hadronize at the phase boundary. For a detailed discussion of this point see Andronic *et al.* (2008).

The most recent data from the RHIC accelerator provide interesting new insight into the connection between QGP formation and charmonium production but the
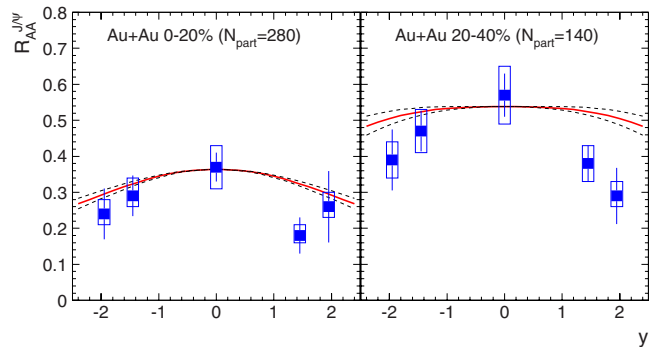

FIG. 15. (Color online) Rapidity dependence of the nuclear modification factor $R_{AA}^{J/\psi}$ for two centrality classes. The data (symbols with errors) are compared to calculations (lines). The dashed lines result from uncertainties in the J/ψ distribution in proton-proton collisions. From Adare *et al.*, 2007.

question how to use charmonia as messengers of deconfinement is far from settled. Here we briefly describe the surprising aspects of the new PHENIX data and argue that they lend first support to the regeneration scenario described above. The major new insight came from a study of the rapidity[26] and centrality dependence (measured through the number of participating nucleons in the collision) of the nuclear modification factor $R_{AA}^{J/\psi}$ which has, for the first time, been measured by the PHENIX Collaboration (Adare *et al.*, 2007) in Au-Au collisions. This modification factor for J/ψ production is defined as

$$R_{AA}^{J/\psi} = \frac{dN_{J/\psi}^{\mathrm{AuAu}}/dy}{N_{\mathrm{coll}}\, dN_{J/\psi}^{pp}/dy} \qquad (17)$$

and relates the charmonium yield in nucleus-nucleus collisions to that expected for a superposition of independent nucleon-nucleon collisions. Here $dN_{J/\psi}/dy$ is the rapidity density of the J/ψ yield for AA and pp collisions and N_{coll} is the number of binary nucleon-nucleon collisions for a given centrality class.

In Fig. 15 we present the new data from the PHENIX Collaboration (Adare *et al.*, 2007). The most striking feature of these data is the observation of a maximum in the rapidity dependence of $R_{AA}^{J/\psi}$ at midrapidity (corresponding to $y=0$, i.e., production perpendicular to the beam direction). This maximum was entirely unexpected as the observed trend is opposite to that expected from the melting model (Matsui and Satz, 1986; Satz, 2006), where $R_{AA}^{J/\psi}$ should attain its smallest value (maximum suppression) in regions of phase space with maximum energy density, i.e., near midrapidity. Likewise, the destruction of charmonia by comoving hadrons would also lead to the largest suppression at midrapidity, in conflict with PHENIX data.

---

[26]The "rapidity" of a particle is defined through its total energy E and the longitudinal momentum p_z along the beam axis as $y = \frac{1}{2}\ln[(E+p_z)/(E-p_z)]$. In contrast to a particle's velocity its rapidity y is additive under Lorentz transformations.
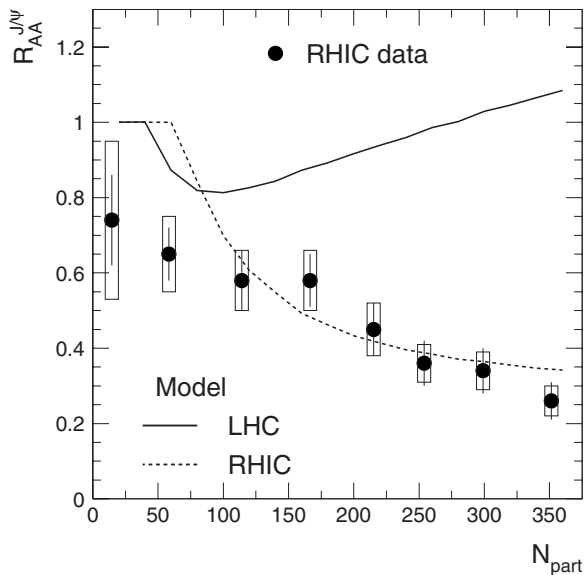
FIG. 16. Centrality dependence of the nuclear modification factor $R_{AA}^{J/\psi}$ for RHIC and LHC energies. The RHIC data are from the PHENIX experiment. The calculations are performed within the framework of the statistical hadronization model (Andronic *et al.*, 2007a, 2007b). From Adare *et al.*, 2007.

On the other hand, the observed maximum of $R_{AA}^{J/\psi}$ at midrapidity is naturally explained in the recombination model of Andronic *et al.* (2007a) as due to enhanced charmonium production at the phase boundary: the number of charm quarks is maximal at midrapidity and this maximum is enhanced even further through recombination. This mechanism provides a good description of the data, as indicated by the curves in Fig. 15. In this sense, the PHENIX measurement constitutes first evidence for the statistical production of J/ψ at chemical freeze-out. Further support for this interpretation comes from the observed centrality dependence of $R_{AA}^{J/\psi}$ at midrapidity as shown in Fig. 16. We reiterate that if the recombination model is correct, it implies complete charmonium quenching in the QGP, as discussed above.

One should note that, at present, there are also other interpretations of the PHENIX data, in particular, through cold nuclear matter effects possibly reducing the number of gluons and, hence, charm quarks when going away from midrapidity. Precision data on J/ψ production and its possible hydrodynamic flow will be needed to distinguish between these different descriptions. The situation has been reviewed by Granier de Cassagnac (2008).

Since the number of charm quark pairs is still rather moderate at RHIC energies, a strong enhancement of J/ψ production is not expected in the PHENIX measurement. The model predictions reproduce very well the decreasing trend versus centrality seen in the RHIC data (Adare *et al.*, 2007). In contrast, at the much higher LHC energy, the charm production cross section is expected to be about an order of magnitude larger (Vogt, 2003). As a result, a totally opposite trend as a function

of centrality is predicted (Fig. 16) with R_{AA} exceeding 1 for central collisions.

For these predictions it is assumed that charm quarks are effectively thermalized in the very hot and dense QGP, implying that their recombination at the phase boundary gives rise to a significant increase in yield near midrapidity. As shown, the resulting predictions for measurements at LHC energies lead to a rather dramatic enhancement rather than suppression in central Pb-Pb collisions. If observed, this would be a spectacular fingerprint of a high-energy quark-gluon plasma, in which charm quarks are effectively deconfined. The data on charmonium production in Pb-Pb collisions from the LHC will be decisive in settling the issue.

V. PHASES AT HIGH BARYON DENSITY

Nuclear matter can be compressed in two distinctly different ways: a rapid squeeze that leads to strong heating, as realized in heavy-ion collisions at relativistic energies; a slow squeeze which results in cold matter at very high baryon density. This type of compression is impossible to achieve in the laboratory but is realized in the interior of a neutron star, a few seconds after it has been born in a supernova explosion. It is conceivable that, in the inner core, densities as high as ten times that in the middle of a heavy nucleus can be reached (Lattimer and Prakash, 2007). Under such conditions it is expected that the closely packed neutrons (with a small admixture of protons, electrons, and muons as well as baryons carrying strange quarks) dissolve into their constituents and the u, d, s quarks form a degenerate Fermi liquid.[27] The composition is determined by charge and color neutrality and the requirement of β equilibrium, i.e., equilibrium of weak interaction processes.

It has long been known that fermionic systems at low temperatures become unstable to the formation and condensation of "Cooper pairs" if the interaction between two fermions is attractive. This situation is expected in quark-gluon matter above the deconfinement transition (Frautschi, 1971; Barrois, 1977). Here the Cooper instability of the Fermi surface and the formation of di-quark pairs is mediated by the attractive interaction induced by gluon exchange between two quarks of specific color, flavor and spin combinations. Since such combinations carry net color, the new state is called a "color superconductor," a term that was first used by Frautschi (1971) and Barrois (1977). The presence of color superconductivity in the core of neutron stars could lead to interesting new effects in the long-time evolution of such objects such as modifications of the cooling rate through neutrino emission, instabilities caused by gravitational wave radiation of pulsars, or glitches in the spin-down rate (Alford *et al.*, 2008).

---

[27] Because of their much larger (Higgs) masses charm, bottom and top quarks play no role at the relevant densities.

A. Color superconductivity

Early analysis of the possible pairing patterns in cold quark matter and estimates of the resulting gaps Δ based on the exchange of a single gluon (Bailin and Love, 1979, 1984) led to values of a few MeV for Δ. Such low values have little influence on the high-density EoS. This situation changed in the 1990s when it was pointed out that in the physically interesting region of μ_q ~ 500 MeV, which corresponds to about ten times the density in a heavy nucleus, perturbative one-gluon exchange is inadequate because of the strong increase in α_s at such momentum scales. The resulting nonperturbative effects in the quark-gluon coupling were estimated in the NJL model and led to gap values of up to 100 MeV (Alford *et al.*, 1998; Rapp *et al.*, 1998). Subsequently, it was found that the many possible combinations of flavor-color and spin degrees of freedom, dictated by the fermionic antisymmetry of the Cooper pair wave function, can lead to a rich phase structure (Rischke, 2004; Buballa, 2005; Alford *et al.*, 2007). For total spin $S=0$ one has the possibility of pairing two quark flavors, say up or down, leaving the third flavor unpaired (the so-called "2SC" phase) or all three quark flavors can participate. In this case there is a definite combination of color and flavor degrees of freedom called "color-flavor locking" (CFL). Under the conditions of charge and color neutrality as well as β equilibrium the Fermi energies of quarks with given color and flavor quantum numbers are in general not equal. The imbalance is partly caused by the mass difference $m_s - m_{u,d}$. For a large mismatch, pairing with unequal quantum numbers becomes difficult "stressed superconductivity" and can even lead to "gapless" phases [g2SC (Shovkovy and Huang, 2003) and gCFL (Alford *et al.*, 2004)]. Also crystalline phases similar to the Larkin-Ovchinnikov-Fulde-Ferrell phases (Fulde and Ferrell, 1964; Larkin and Ovchinnikov, 1965) in conventional superconductors are conceivable (Alford *et al.*, 2007). Which phase is favored at a given temperature and density is determined by the global minimum of the free energy. An example is shown in Fig. 17. Comparing Figs. 11 and 17 it is unlikely that any of the high-density and low-temperature phases can be explored in heavy-ion collisions.

Stressed superconductivity can however be studied experimentally in trapped ultracold fermionic atomic gases (Giorgini *et al.*, 2008). Here an imbalance in chemical potentials can be achieved by populating two hyperfine states of the atom with a different number of particles. At the same time the interaction strength can be controlled using Feshbach resonances, to drive the system from weak coupling (BCS regime) through the point where diatomic bound states form to the point where diatomic molecules undergo Bose-Einstein condensation (BEC regime). Thus many of the predicted phases of cold quark matter can be "simulated" in the laboratory with interesting future perspectives and cross fertilization.
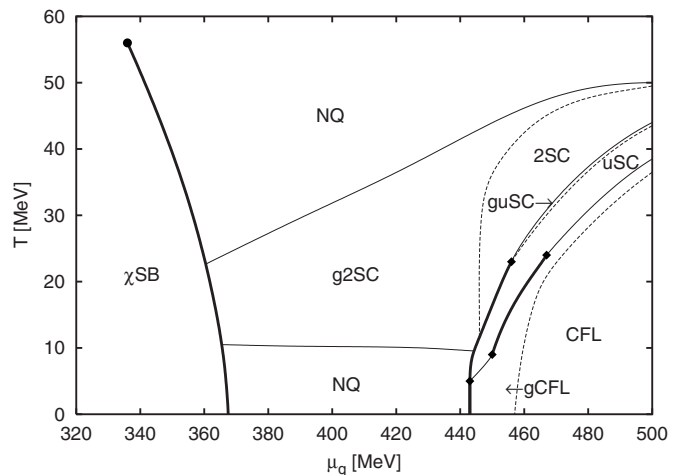

FIG. 17. Color superconducting phases at high baryochemical potential $\mu_q = \mu_b/3$ and low temperatures as predicted by the NJL model in the Hartree approximation. The region of spontaneously broken chiral symmetry is denoted by χSB while regions where quark matter is in the normal state are indicated by NQ. The bold solid lines mark boundaries of first-order transitions, while the thin lines denote second-order boundaries. The dashed lines indicate the boundaries between gapless and gapped regions. Several critical points are found. From Ruster *et al.*, 2005.

Even though the NJL model is useful in exploring the many possibilities of superconducting phases, its quantitative predictive power is limited by the large sensitivity of the results to the model parameters. First-principles calculations, on the other hand, are very difficult since they require accurate knowledge of the di-quark interaction on scales of the Fermi energy ϵ_F where α_s is large. Only at very high densities or asymptotically large μ_q, the coupling becomes small enough to make reliable predictions from first principles. In this case one-gluon exchange between di-quarks dominates. In the dense medium its longitudinal (color-electric) component is Debye screened while the transversal (color-magnetic) components are dynamically screened due to Landau damping. This implies that the ratio of the magnetic to electric polarization functions goes like $\omega/|\vec{q}|$, where ω is the frequency and $\vec{q}$ is the three-momentum of the gluon field. In the static limit $\omega \rightarrow 0$ the magnetic components therefore remain unscreened. As a consequence, in contrast to the usual BCS theory where the pairing gap as a function of the coupling constant g varies as Δ/μ $\sim \exp(-\text{const}/g^2)$, one has (Son, 1999)

$$\Delta/\mu_q \sim \exp(-3\pi^2/\sqrt{2}g_s). \tag{18}$$

Such retardation effects for long-range forces are also known in condensed matter physics (Eliashberg, 1960, 1961). The $1/g_s$ dependence in the exponent of the gap function leads to the surprising phenomenon that the pairing gap can take arbitrarily large values, even though the coupling decreases (Rajagopal and Wilczek,

2001).[28] Taking into account the color-flavor-spin degrees of freedom one finds the CFL phase to be the energetically most favored pairing state at asymptotically large quark chemical potentials (Fig. 17).

Even though these *ab initio* findings are interesting from a many-body point of view, they are valid only for asymptotically large values of μ_q because of the logarithmic running of α_s [Eq. (9)].[29] Hence, they are of little relevance for the interior of neutron stars where $\mu_q \sim 400$–600 MeV. One can try to remedy this by inclusion of higher-order corrections in g_s. Since at such scales $g_s \simeq 1$ it is questionable, however, whether such perturbative expansion schemes are justified. A more promising approach is to use Schwinger-Dyson equations where both the quark and gluon fields are treated nonperturbatively with a proper treatment of infrared (small-momentum behavior) of α_s. Recent results (Nickel, Alkofer, and Wambach, 2006; Nickel, Wambach, and Alkofer, 2006) indicate that in the relevant regime of quark densities in the core of neutron stars pairing gaps of the order of 100 MeV can be expected, confirming the earlier findings within NJL model studies.

VI. SUMMARY AND CONCLUSIONS

In the 30 years since the first discussions about the phases of QCD and the corresponding phase diagram there has been tremendous progress in our understanding of strongly interacting matter at extreme conditions. Large experimental campaigns have been mounted and have amassed a wealth of new data and led to a series of discoveries. Here we have concentrated on aspects relevant to the QCD phase diagram. In particular, we have discussed that for symmetric matter ($\mu_b = 0$) the chemical freeze-out temperature can be determined with an uncertainty of better than 10% from measured hadron abundances. We have further argued that the observed temperature behavior lends strong support to the notion of a critical temperature T_H introduced by Hagedorn and provided arguments that T_H coincides with T_c, the critical temperature for the quark-hadron transition of strongly interacting matter. Thus an important point in the phase diagram has been established experimentally. We have furthermore summarized the evidence for mass changes of hadrons near the phase boundary, with particular emphasis on the ρ meson and laid out arguments how these findings are connected to the restoration of chiral symmetry near the phase transition line. Charmonium production is apparently strongly influenced by the QCD phase transition and we have outlined the particular role of this production process for studies of decon-

finement. Along with the experimental progress also came impressive theoretical developments, both concerning "exact" solutions of QCD on a discrete space-time lattice, as well as the development of powerful effective models to study the physical processes emerging from the experimental observations.

What may be expected in the future? With the experimental program at RHIC and in particular the heavy-ion program at the CERN LHC[30] the structure of the matter above T_c and at vanishing chemical potential can be studied quantitatively. In particular, the fireballs formed in Pb-Pb collisions at LHC energies will have much higher initial temperatures, maybe reaching 1 GeV, and live much longer (>10 fm lifetime up to the quark-hadron phase transition) than those produced at RHIC. Furthermore, hard probes, in particular high transverse-momentum jets and heavy quarks, will be abundantly produced. From studies in this new environment should emerge not only detailed tests of *ab initio* QCD predictions about the phase transition as well as information about the bulk properties of the QGP at high temperature and its stopping power for high-momentum quarks but also insight into the nature of the processes that lead to confinement. Studies of the phases of strongly interacting matter at high densities and moderate temperatures, on the other hand, are still in their infancy. The development of relevant effective theories (including the complex reaction dynamics) as well as developments of lattice QCD simulations at finite chemical potentials are important milestones in the understanding of quark matter at high densities. Further experimental studies at lower energy at the RHIC collider as well as with the planned CBM experiment at the FAIR facility at GSI are mandatory to make progress in our understanding of the QCD phase transition in the high-density regime.

REFERENCES

Abelev, B. I., *et al.* (STAR), 2007, Phys. Rev. Lett. **98**, 192301.

Abreu, M. C., *et al.* (NA50), 2001, Phys. Lett. B **521**, 195.

Adamova, D., *et al.*, (CERES/NA45), 2003, Phys. Rev. Lett. **91**, 042301.

Adamova, D., *et al.*, 2008, Phys. Lett. B **666**, 425.

Adams, J., *et al.* (STAR), 2005a, Phys. Rev. C **72**, 014904.

Adams, J., *et al.* (STAR), 2005b, Nucl. Phys. A **757**, 102.

Adare, A., *et al.* (PHENIX), 2007, Phys. Rev. Lett. **98**, 232301.

Adcox, K., *et al.* (PHENIX), 2005, Nucl. Phys. A **757**, 184.

Adler, S. S., *et al.* (PHENIX), 2006a, Phys. Rev. Lett. **97**, 052301.

Adler, S. S., *et al.* (PHENIX), 2006b, Phys. Rev. Lett. **96**,

---

[28]Note that $g_s = \sqrt{4\pi\alpha_s}$ according to Eq. (9) behaves like $\sqrt{1/\ln \mu_q}$ if one assumes that the momentum scale Q is governed by μ_q. Inserting this into Eq. (18) it is clear that the exponential drops more slowly than $1/\mu_q$.

[29]For weak coupling theory to apply in QCD μ_q has to be of the order of 10^4 MeV (Fig. 2).

---

[30]The LHC is now scheduled to start operations in the summer of 2009, first with protons and afterwards with a pilot run for the Pb beam program.

032301.

Adler, S. S., *et al.* (PHENIX), 2007, Phys. Rev. C **76**, 034904.

Afanasiev, S., *et al.* (PHENIX), 2007, e-print arXiv:0706.3034.

Agakichiev, G., *et al.*, 1995, Phys. Rev. Lett. **75**, 1272.

Agakichiev, G., *et al.* (CERES), 2005, Eur. Phys. J. C **41**, 475.

Agakichiev, G., *et al.* (HADES), 2007, Phys. Rev. Lett. **98**, 052302.

Agakishiev, G., *et al.* (CERES/NA45), 1998, Phys. Lett. B **422**, 405.

Agakishiev, G., *et al.* (HADES), 2008, Phys. Lett. B **663**, 43.

Akiba, Y. (PHENIX), 2006, Nucl. Phys. A **774**, 403.

Alford, M., C. Kouvaris, and K. Rajagopal, 2004, Phys. Rev. Lett. **92**, 222001.

Alford, M. G., K. Rajagopal, and F. Wilczek, 1998, Phys. Lett. B **422**, 247.

Alford, M. G., A. Schmitt, K. Rajagopal, and T. Schafer, 2008, Rev. Mod. Phys. **80**, 1455.

Allton, C. R., *et al.*, 2003, Phys. Rev. D **68**, 014507.

Andronic, A., F. Beutler, P. Braun-Munzinger, K. Redlich, and J. Stachel, 2009, Phys. Lett. B **675**, 312.

Andronic, A., P. Braun-Munzinger, K. Redlich, and J. Stachel, 2007a, Phys. Lett. B **652**, 259.

Andronic, A., P. Braun-Munzinger, K. Redlich, and J. Stachel, 2007b, Nucl. Phys. A **789**, 334.

Andronic, A., P. Braun-Munzinger, K. Redlich, and J. Stachel, 2008, Phys. Lett. B **659**, 149.

Andronic, A., P. Braun-Munzinger, and J. Stachel, 2006, Nucl. Phys. A **772**, 167.

Angelis, A. L. S., *et al.* (HELIOS-3), 1998, Eur. Phys. J. C **5**, 63.

Aoki, Y., G. Endrodi, Z. Fodor, S. D. Katz, and K. K. Szabo, 2006, Nature (London) **443**, 675.

Aoki, Y., Z. Fodor, S. D. Katz, and K. K. Szabo, 2006, Phys. Lett. B **643**, 46.

Applegate, J. H., C. J. Hogan, and R. J. Scherrer, 1988, Astrophys. J. **329**, 572.

Arnaldi, R., *et al.* (NA60), 2006, Phys. Rev. Lett. **96**, 162302.

Arsene, I., *et al.* (BRAHMS), 2005, Nucl. Phys. A **757**, 1.

Back, B. B., *et al.*, 2005, Nucl. Phys. A **757**, 28.

Bailin, D., and A. Love, 1979, J. Phys. A **12**, L283.

Bailin, D., and A. Love, 1984, Phys. Rep. **107**, 325.

Bardeen, J., L. N. Cooper, and J. R. Schrieffer, 1957, Phys. Rev. **108**, 1175.

Barrois, B. C., 1977, Nucl. Phys. B **129**, 390.

Becattini, F., 1996, Z. Phys. C **69**, 485.

Becattini, F., P. Castorina, J. Manninen, and H. Satz, 2008, Eur. Phys. J. C **56**, 493.

Becattini, F., M. Gazdzicki, A. Keranen, J. Manninen, and R. Stock, 2004, Phys. Rev. C **69**, 024905.

Becattini, F., and U. W. Heinz, 1997, Z. Phys. C **76**, 269.

Becattini, F., J. Manninen, and M. Gazdzicki, 2006, Phys. Rev. C **73**, 044905.

Bethke, S., 2007, Prog. Part. Nucl. Phys. **58**, 351.

Blaizot, J.-P., A. Ipp, and A. Rebhan, 2006, Ann. Phys. (N.Y.) **321**, 2128.

Boyanovsky, D., H. J. de Vega, and D. J. Schwarz, 2006, Annu. Rev. Nucl. Part. Sci. **56**, 441.

Braun-Munzinger, P., K. Redlich, and J. Stachel, 2004, *Particle Production in Heavy Ion Collisions* (World Scientific, Singapore).

Braun-Munzinger, P., and J. Stachel, 1996, Nucl. Phys. A **606**, 320.

Braun-Munzinger, P., and J. Stachel, 1998, Nucl. Phys. A **638**, 3.

Braun-Munzinger, P., and J. Stachel, 2000, Phys. Lett. B **490**, 196.

Braun-Munzinger, P., and J. Stachel, 2001, Nucl. Phys. A **690**, 119.

Braun-Munzinger, P., and J. Stachel, 2002, J. Phys. G **28**, 1971.

Braun-Munzinger, P., and J. Stachel, 2007, Nature (London) **448**, 302.

Braun-Munzinger, P., J. Stachel, J. P. Wessels, and N. Xu, 1996, Phys. Lett. B **365**, 1.

Braun-Munzinger, P., J. Stachel, and C. Wetterich, 2004, Phys. Lett. B **596**, 61.

Braun-Munzinger, P., and J. Wambach, 2006, Physik J. **5**, 41.

Brown, G. E., 1988, Nucl. Phys. A **488**, 689c.

Brown, G. E., J. W. Holt, C.-H. Lee, and M. Rho, 2007, Phys. Rep. **439**, 161.

Brown, G. E., and M. Rho, 1991, Phys. Rev. Lett. **66**, 2720.

Buballa, M., 2005, Phys. Rep. **407**, 205.

Cabibbo, N., and G. Parisi, 1975, Phys. Lett. **59B**, 67.

Capella, A., A. B. Kaidalov, and D. Sousa, 2002, Phys. Rev. C **65**, 054908.

Casalderrey-Solana, J., E. V. Shuryak, and D. Teaney, 2005, J. Phys.: Conf. Ser. **27**, 22.

Chandrasekhar, S., 1931, Astrophys. J. **74**, 81.

Chaplin, M., 2007, www.lsbu.ac.uk/water/phase.html

Cheng, M., *et al.*, 2006, Phys. Rev. D **74**, 054507.

Chodos, A., R. L. Jaffe, K. Johnson, C. B. Thorn, and V. F. Weisskopf, 1974, Phys. Rev. D **9**, 3471.

Cleymans, J., and K. Redlich, 1998, Phys. Rev. Lett. **81**, 5284.

Collins, J. C., and M. J. Perry, 1975, Phys. Rev. Lett. **34**, 1353.

de Forcrand, P., and O. Philipsen, 2002, Nucl. Phys. B **642**, 290.

Dey, M., V. L. Eletsky, and B. L. Ioffe, 1990, Phys. Lett. B **252**, 620.

Dokshitzer, Y. L., and D. E. Kharzeev, 2001, Phys. Lett. B **519**, 199.

Eliashberg, G. M., 1960, Sov. Phys. JETP **11**, 696.

Eliashberg, G. M., 1961, Sov. Phys. JETP **12**, 1000.

Feinberg, E. L., 1976, Nuovo Cimento A **34**, 391.

Fischer, C. S., 2006, J. Phys. G **32**, R253.

Fisher, M. E., 1967, Physics (Long Island City, N.Y.) **3**, 255.

Fodor, Z., and S. D. Katz, 2002, Phys. Lett. B **534**, 87.

Fodor, Z., and S. D. Katz, 2004, J. High Energy Phys. **2004**, 050.

Fortov, V. E., R. I. Ilkaev, V. A. Arinin, V. V. Burtzev, V. A. Golubev, I. L. Iosilevskiy, V. V. Khrustalev, A. L. Mikhailov, M. A. Mochalov, V. Y. Ternovoi, and M. V. Zhernokletov, 2007, Phys. Rev. Lett. **99**, 185001.

Frautschi, S. C., 1971, Phys. Rev. D **3**, 2821.

Frautschi, S. C., 1978, in *Proceedings of the Workshop on Hadronic Matter at Extreme Energy Density*, edited by N. Cabbibo (Erice Hadronic Matter, Erice, Italy).

Fritzsch, H., M. Gell-Mann, and H. Leutwyler, 1973, Phys. Lett. **47B**, 365.

Fromerth, M. J., and J. Rafelski, 2002, e-print arXiv:astro-ph/0211346.

Fulde, P., and R. A. Ferrell, 1964, Phys. Rev. **135**, A550.

Gallmeister, K., B. Kämpfer, O. Pavlenko, and C. Gale, 2001, Nucl. Phys. A **688**, 939.

Gavin, S., and R. Vogt, 1997, Phys. Rev. Lett. **78**, 1006.

Gebhard, F., 1997, *The Mott Metal-Insulator Transition* (Springer, Berlin).

Giorgini, S., L. P. Pitaevskii, and S. Stringari, 2008, Rev. Mod. Phys. **80**, 1215.

Goldstone, J., 1961, Nuovo Cimento **19**, 154.

Granier de Cassagnac, R., 2008, J. Phys. G **35**, 104023.

Greenberg, O. W., 1964, Phys. Rev. Lett. **13**, 598.

Gross, D. J., and F. Wilczek, 1973, Phys. Rev. Lett. **30**, 1343.

Gyulassy, M., and L. McLerran, 2005, Nucl. Phys. A **750**, 30.

Hagedorn, R., 1965, Nuovo Cimento, Suppl. **3**, 147.

Heckmann, K., 2007, private communication.

Heinz, U., and G. Kestin, 2006, in *Critical Point and Onset of Deconfinement*, Proceedings of Science (SISSA, Trieste), 038.

Heinz, U. W., 1998, Nucl. Phys. A **638**, 357c.

Huang, K., and S. Weinberg, 1970, Phys. Rev. Lett. **25**, 895.

Huovinen, P., P. F. Kolb, U. W. Heinz, P. V. Ruuskanen, and S. A. Voloshin, 2001, Phys. Lett. B **503**, 58.

Itoh, N., 1970, Prog. Theor. Phys. **44**, 291.

Kämpfer, B., 2007, private communication.

Kampfer, B., M. Bluhm, H. Schade, R. Schulze, and D. Seipt, 2007, e-print arXiv:0708.3322.

Kapusta, J. I., and E. V. Shuryak, 1994, Phys. Rev. D **49**, 4694.

Karsch, F., 2002, Lect. Notes Phys. **583**, 209.

Karsch, F., K. Redlich, and L. Turko, 1993, Z. Phys. C **60**, 519.

Kolb, P., and U. Heinz, 2004, in *Quark-Gluon Plasma3*, edited by R. Hwa, and X. Wang (World Scientific, Singapore), pp. 634–714.

Larkin, A. I., and Y. N. Ovchinnikov, 1965, Sov. Phys. JETP **20**, 762.

Lattimer, J. M., and M. Prakash, 2007, Phys. Rep. **442**, 109.

Matsui, T., and H. Satz, 1986, Phys. Lett. B **178**, 416.

Mott, N. F., 1968, Rev. Mod. Phys. **40**, 677.

Mrowczynski, S., and M. H. Thoma, 2007, Annu. Rev. Nucl. Part. Sci. **57**, 61.

Nambu, Y., 1960, Phys. Rev. Lett. **4**, 380.

Nambu, Y., and G. Jona-Lasinio, 1961a, Phys. Rev. **122**, 345.

Nambu, Y., and G. Jona-Lasinio, 1961b, Phys. Rev. **124**, 246.

Nickel, D., R. Alkofer, and J. Wambach, 2006, Phys. Rev. D **74**, 114015.

Nickel, D., J. Wambach, and R. Alkofer, 2006, Phys. Rev. D **73**, 114028.

O'Hara, K. M., S. L. Hemmer, M. E. Gehm, S. R. Granade, and J. E. Thomas, 2002, Science **298**, 2179.

Philipsen, O., 2006, *XXIIIrd International Symposium on Lattice Field Theory*, Proceedings of Science (SISSA, Trieste), 016.

Philipsen, O., 2007, e-print arXiv:0710.1217.

Pisarski, R. D., 1982, Phys. Lett. **110B**, 155.

Politzer, H. D., 1973, Phys. Rev. Lett. **30**, 1346.

Porter, R. J., *et al.* (DLS), 1997, Phys. Rev. Lett. **79**, 1229.

Proc. Quark-Matter 2005 Conference, 2006, Nucl. Phys. A 774, 1.

Proc. Quark-Matter 2006 Conference, 2007, J. Phys. G 34, 1.

Proc. Quark-Matter 2008 Conference, 2008, J. Phys. G 35, 1.

Proceedings of Science, 2006, CPOD 2006, 1.

Rafelski, J., and J. Letessier, 2008, J. Phys. G **35**, 044042.

Rajagopal, K., and F. Wilczek, 2001, *At the Frontier of Particle Physics/Handbook of QCD* (World Scientific, Singapore), pp. 2061–2151.

Rapp, R., T. Schafer, E. V. Shuryak, and M. Velkovsky, 1998, Phys. Rev. Lett. **81**, 53.

Rapp, R., and J. Wambach, 1999, Eur. Phys. J. A **6**, 415.

Rapp, R., and J. Wambach, 2000, Adv. Nucl. Phys. **25**, 1.

Rischke, D. H., 2004, Prog. Part. Nucl. Phys. **52**, 197.

Roche, G., *et al.* (DLS), 1989, Phys. Lett. B **226**, 228.

Ruster, S. B., V. Werth, M. Buballa, I. A. Shovkovy, and D. H. Rischke, 2005, Phys. Rev. D **72**, 034004.

Satz, H., 2006, J. Phys. G **32**, R25.

Schwarz, D. J., 1998, Mod. Phys. Lett. A **13**, 2771.

Shapiro, S. L., and S. A. Teukolsky, 1983, *Black Holes, White Dwarfs and Neutron Stars* (Wiley, New York).

Shovkovy, I., and M. Huang, 2003, Phys. Lett. B **564**, 205.

Shuryak, E. V., 1978, Phys. Lett. **78B**, 150.

Son, D. T., 1999, Phys. Rev. D **59**, 094019.

Specht, H. J., 2008, Nucl. Phys. A **805**, 338.

Spieles, C., *et al.*, 1999, Phys. Rev. C **60**, 054901.

Stephanov, M. A., 2004, Prog. Theor. Phys. Suppl. **153**, 139.

Stock, R., 1999, Phys. Lett. B **456**, 277.

Stoecker, H., 2005, Nucl. Phys. A **750**, 121.

Teaney, D., J. Lauret, and E. V. Shuryak, 2002, Nucl. Phys. A **698**, 479.

Thews, R. L., M. Schroedter, and J. Rafelski, 2001, Phys. Rev. C **63**, 054905.

Thomas, D., D. N. Schramm, K. A. Olive, and B. D. Fields, 1993, Astrophys. J. **406**, 569.

van Hees, H., and R. Rapp, 2006, Phys. Rev. Lett. **97**, 102301.

van Hees, H., and R. Rapp, 2007, private communication.

van Hees, H., and R. Rapp, 2008, Nucl. Phys. A **806**, 339.

Vitev, I., 2006, J. Phys.: Conf. Ser. **50**, 119.

Vogt, R. (Hard Probe), 2003, Int. J. Mod. Phys. E **12**, 211.

Weinberg, S., 1967, Phys. Rev. Lett. **18**, 507.

Yang, C.-N., and R. L. Mills, 1954, Phys. Rev. **96**, 191.

Yao, W.-M., *et al.* (Particle Data Group), 2006, J. Phys. G **33**, 1.